

ENGINEERING RESEARCH INSTITUTE  
UNIVERSITY OF MICHIGAN  
ANN ARBOR, MICH.

INFLUENCE OF HEAT TREATMENT  
ON THE  
MICROSTRUCTURE AND HIGH-TEMPERATURE  
PROPERTIES OF A 55 Ni - 20 Cr - 15 Co - 4 Mo - 3 Ti - 3 Al ALLOY

by

R. F. Decker

John P. Rowe

W. C. Bigelow

J. W. Freeman

Report 56

to

THE NATIONAL ADVISORY COMMITTEE FOR AERONAUTICS

January 30, 1957

Project 1478-11

en 81

UMR 0593

## ACKNOWLEDGMENTS

The invaluable contribution of a number of people who have assisted on this project is acknowledged.

Professor C. C. Craig supplied valuable advice about the statistical analysis included in the appendix.

Mr. Karl Kienholz operated the University of Michigan vacuum-melting furnace in the processing of the experimental heats. Mr. Jerry White assisted in hot working and heat treated many of the samples.

Mr. Alex Dano's development of etching procedures for both macroscopic and optical-microscopic work and the subsequent utilization of the techniques by Mr. Dano were instrumental in the completion of the microstructural studies. In addition, Mr. Dano's careful and precise techniques resulted in the electron micrographs shown in the report. Miss Christine Sadler prepared many of the metallographic samples and photographs.

Mr. George Hynes and Mr. Dick Umstead ran the stress-rupture tests.

## SUMMARY

Studies have been made of the influence of various heat treatments on the rupture properties and microstructure of a 55 Ni - 20 Cr - 15 Co - 4 Mo - 3 Ti - 3 Al alloy to provide more fundamental information on the relationships between structure and high-temperature properties in this type of alloy. The effects of variations in solution treatment, cooling rate after solution treatment, and aging treatment on the stress-rupture properties of the alloy at 1600°F and 25,000 psi have been measured and related to variations in the size and distribution of precipitates within the alloy and to residual rolling effects.

The temperature for complete solution of precipitates was found to lie between 1975° and 2000°F, and the temperature at which the alloy was solution treated was found to have a marked effect on its stress-rupture properties. Solution treatment at 1975°F resulted in a shorter rupture life than treatment at 2150°F, or treatment at 2150°F followed by treatment at 1975°F. The experimental evidence indicates that this was not due to the lack of complete solution of the  $\gamma'$  phase but to the fact that residual effects from prior rolling operations remained in the alloy when the 1975°F solution treatment alone was used.

Cooling rate after solution treatment also affected subsequent stress-rupture properties of the alloy. The extremely rapid and extremely slow cooling rates, accompanying ice-brine quenching and furnace cooling, resulted in inferior rupture properties to moderate cooling achieved by air cooling. These effects were related to the distribution of the  $\gamma'$  phase. Furnace cooling caused overaging with a coarse dispersion of agglomerated  $\gamma'$  particles while ice-brine quenching induced considerable cellular precipitation of the  $\gamma'$  phase at the grain boundaries. The inferior properties after these treatments are considered to be manifestations of these overaging phenomena.

Double-aging treatments after solution treatment had no significant effect on stress-rupture properties. Qualitative comparisons were made of the effects of isothermal aging with and without application of stress. No significant difference was noted in the rate at which precipitation of the  $\gamma'$  phase proceeded within the matrix grains. In general, the rate of localized precipitation at the grain boundaries was also similar at part of the grain boundaries; but there appeared to be a higher incidence of severe overaging and agglomeration in restricted portions of grain boundaries in the specimens aged under stress.

In general, it was concluded that the stress-rupture properties of the alloy could be related to the size and dispersion of the  $\gamma'$ , providing that residual rolling effects had been removed by the solution treatment. The heat treatments which left finely dispersed  $\gamma'$  throughout the microstructure gave essentially equal properties at 1600°F and 25,000 psi. Heat treatments which caused overaging in the matrix or at the grain boundaries before testing led to significantly lower high-temperature properties.

## INTRODUCTION

It is generally accepted that the favorable high-temperature properties of the Ti + Al hardened nickel-base alloys result from the precipitation of the intermetallic  $\gamma'$  phase within the matrix of the alloy. The  $\gamma'$  phase has been shown to have a face-centered cubic structure similar to that of the  $\text{Ni}_3\text{Al}$  phase of the nickel-aluminum system with a lattice parameter closely matched to that of the matrix of the alloys (refs. 1 and 2). Compositionally, the phase has been shown to dissolve titanium and is frequently referred to as  $\text{Ni}_3(\text{Al}, \text{Ti})$ . The heat resistance of these alloys has been attributed to the presence of  $\gamma'$  (refs. 1, 3 and 4) and to the fact that  $\gamma'$  forms in fine dispersion within the matrix; however, attempts to relate the distribution of the  $\gamma'$  particles with the metallurgical properties have been only moderately successful to date.

Frey, Freeman, and White (ref. 5) and subsequently Brockway and Bigelow (ref. 6) found that the dispersion of the  $\gamma'$  particles in Inconel-X alloy correlated with stress-rupture properties at 1200°F, which was low in the aging range for this alloy; however, no correlation was obtained for rupture tests at 1500°F, which was high in the aging-temperature range and which produced rapid aging during testing. Betteridge and Smith (ref. 7) studied the relation between structure and creep properties of Nimonic alloys when tested high in the aging range. They found that highest stress-rupture properties were obtained with the greatest volume percent of  $\gamma'$  and showed that usefulness of conventional aging was clearly decreased when test temperature was greater than 1600°F. The absence of a discontinuity in the rupture strength versus temperature curve in the region of the temperature at which the  $\gamma'$  was completely soluble was interpreted as showing that rupture strength was a consequence of both precipitation and solid-solution hardening. This is in agreement with the theories of Geisler (ref. 8) on the effect of age hardening on deformation resistance and with his proposal that the depletion of solid-solution hardeners by overaging can reduce deformation resistance to that of the solutioned alloy.

In order to extend the knowledge of the nickel-base alloys to the higher Ti + Al levels now in use, a program has been devoted to a study of the effect of heat treatment upon properties of a 55 Ni - 20 Cr - 15 Co - 4 Mo - 3 Al - 3 Ti alloy with the objective of establishing the important variables in heat-treating practice and determining the fundamental metallurgical mechanisms by which they influence the properties of the alloy. This has been part of an extensive program of study of the basic mechanisms by which processing variables influence high-temperature properties of Ti + Al hardened nickel-base heat-resistant alloys which has been in progress at the University of Michigan. This report describes studies of the influence of selected heat treatments on the 1600°F rupture properties of this alloy and the progress which has been made to date in relating these properties to microstructures.

The investigation was conducted at the Engineering Research Institute of the University of Michigan under the sponsorship and with the financial assistance of the National Advisory Committee for Aeronautics.

## EXPERIMENTAL PROCEDURES

### Material

The experiments were conducted on an alloy of the following chemical composition (weight percent):

<u>Cr</u>	<u>Co</u>	<u>Mo</u>	<u>Ti</u>	<u>Al</u>	<u>Mn</u>	<u>Si</u>	<u>Fe</u>	<u>Zr</u>	<u>C</u>	<u>B</u>	<u>S</u>	<u>Ni</u>
18.8	15.1	4.15	3.14	3.14	<.10	.10	<.30	.19	.08	.0005	.008	Bal

This heat was melted in the University of Michigan vacuum-melting furnace from virgin stock in a zirconia crucible and was cast into a 10-pound ingot of 2.5-inch diameter. As-cast structures are shown in figure 1. The ingot was homogenized 1 hour at 2300°F, air cooled, surface ground and rolled to 7/8-inch bar stock using 22 passes of approximately 7-percent reduction each, with 10-minute reheats

between passes. The resulting as-rolled bar stock and its microstructure are illustrated in figure 2.

### Metallography

All metallographic samples were mechanically polished through 3/0 paper and then electropolished in a solution of 10 parts of perchloric acid (70 percent) and 90 parts of glacial acetic acid. Electropolishing was carried out at approximately 30 volts with a current density of 0.8 amperes per square inch. Cyclic polishing of 5 seconds on and 5 seconds off was employed for a total period of electrolysis of about 30 seconds.

Samples for optical microscopy were etched with etchant A (see table I) at 1 to 6 volts with a current density of 0.1 to 0.5 amperes per square inch for 5 to 15 seconds, depending upon the condition of the stock.

Etching for all except one of the electron microstructures was accomplished with a procedure developed by Bigelow, Amy and Brockway (ref. 9) with etchant B (see table I) using 6 volts and a current density of 0.8 amperes per square inch for periods of 3 to 7 seconds. This etching procedure selectively attacks the matrix, leaving the  $\gamma'$  phase protruding from the sample surface. In order to reveal the two-phase composition of the precipitates at the grain boundaries of one of the samples (in figure 18d), etchant B was diluted by a water addition equal to 15% by volume of the original etchant. This was designated as etchant C (see table I). Etchant C causes the carbides to protrude from the sample surface more than the  $\gamma'$ .

For electron microscopy, collodion replicas of the metallic surface were used. These were shadowed with palladium to increase contrast and reveal surface contours; polystyrene latex spheres of approximately  $2580 \text{ \AA}$  in diameter were placed on the replicas prior to shadowing to indicate the angle and direction of shadowing and to provide an internal standard for measurement of magnification. The micrographs reproduced in this report are copies of direct prints from

the original negatives; consequently, the polystyrene spheres appear black and the "shadows" formed by the palladium appear white.

### Hardness

Vickers penetration hardness (VPN) was measured with a 50,000 gram load. Three impressions were made on each sample; both diagonals of each impression being measured. Statistical analysis of testing variability (see appendix) established that in the range of 300 to 340 VPN a hardness difference of 7 VPN was significant while in the range of 340 to 400 VPN a hardness difference of 9 VPN was significant.

### X-Ray Diffraction

X-Ray diffraction studies were made on selected samples to detect the presence of the  $\gamma'$  phase. Samples etched as for electron micrography were mounted on a rotating specimen mount at the center of a Debye-Scherrer-type camera with incident beam at an angle of  $20^\circ$  to the surface. Cr-K radiation was used to give maximum separation of the diffraction lines and to minimize fluorescence effects.

### Stress-Rupture Testing

High-temperature properties were evaluated by stress-rupture tests at  $1600^\circ\text{F}$  and 25,000 psi using 0.250-inch diameter test specimens machined from heat-treated bar stock. The specimens were preheated 4 hours at  $1600^\circ\text{F}$  in the rupture units before the loading.

## RESULTS

The studies of the effect of thermal treatments on the size and distribution of precipitates and on high-temperature properties can be categorized as: (1) study of effect of solution-treating temperature; (2) study of effect of cooling rate after solution treatment; and (3) study of isothermal aging after solution treatment. The

results and discussion will be presented in this order below. The initial microstructures of the rupture samples are presented in figure 3, and the results of rupture tests are plotted on a rupture band in figure 4 and listed in table II. Table III includes the hardness data of the heat treated samples.

#### Effect of Solution-Treating Temperatures

In order to establish the minimum temperature for complete solution of the precipitates in 4 hours, specimens which had been treated 2 hours at 2150°F and air cooled were subsequently treated 4 hours at 1700°, 1800°, 1900° and 2000°F and ice-brine quenched. The initial 2-hour treatment was applied to homogenize the as-rolled structure.

The micrographs of figure 5a, 5b, and 5c show a uniform distribution of the  $\gamma'$  particles throughout the matrix of the alloy. Following the convention of Geisler, this will be referred to henceforth as "general precipitate." From micrographs it appears that the size of the particles increased, but that the volume percent of the phase decreased up to 1900°F. The  $\gamma'$  particles were not evident after treatment at 2000°F.

In the electron micrographs, there is some evidence that two phases agglomerated in the grain boundaries during treatment at 1700°, 1800°, and 1900°F. Particles of one phase were surrounded by a second agglomerated phase. Selective etching techniques (ref. 9) showed that the surrounding phase etched like the general precipitate of  $\gamma'$ . The surrounded particles were distributed less uniformly in the boundaries and are assumed to be carbides.

X-Ray diffraction data obtained provided evidence that  $\gamma'$  was present in the 1900°F sample; however,  $\gamma'$  was not detected in the sample treated at 2000°F (see table IV). This is consistent with the observations on the microstructure described above. Microstructural studies also showed that the solution of the  $\gamma'$  phase was not complete at 1975°F. This was indicated by the occurrence of very large  $\gamma'$  particles,



similar to those in the specimen treated at 1900°F, in a specimen which was treated 2 hours at 2150°F and then reheated 4 hours at 1975°F (see fig. 3c). The presence of the numerous very small  $\gamma'$  particles in figure 3c in addition to these large particles is attributed to the fact that the specimen was air cooled following the 1975°F treatment.

The hardness measurements (fig. 6) confirm the microstructural findings in an indirect way. As the heat-treating temperature was increased to 1900°F, hardness decreased. The hardness after treating at 2000° or 2150°F was, however, significantly higher than the value for 1900°F.

There are believed to be two mechanisms to account for this latter increase in hardness. It could be that matrix solid-solution hardening resulted from dissolving the precipitates ( $\gamma'$  and/or carbides), or that the more complete solution of precipitates obtained at 2000°F created a greater driving force for re-precipitation of the  $\gamma'$  phase during the ice-brine quenching treatment. Regardless, the true hardness indicator of the solution temperature seems to be the sharp increase of hardness between 1900° and 2000°F.

This definitely established the temperature for complete solution of the  $\gamma'$  phase in this alloy as lying between 1975° and 2000°F for a 4-hour treatment. These results are in good agreement with the results of Betteridge and Franklin (ref. 3) on Nimonic alloys containing titanium and aluminum in a 2:1 ratio, if it is assumed that the total percent of Ti + Al is the factor determining the solution temperature. The solution temperature they observed for an alloy containing a total of 6.3% Ti + Al was in the same range as observed here with a comparable Ti + Al content as shown in figure 7.

The micrographs do not show appreciable grain-boundary precipitation in specimens treated in the range of 1975° to 2000°F, indicating that the carbides which generally form at the grain boundaries also dissolve.

### Variation of Stress-Rupture Properties with Solution Treatment

To find the effect of solution treatment on the high-temperature properties, as-rolled samples were heat treated and rupture tested at 1600°F and 25,000 psi. The results, as extracted from table III, are tabulated below and are:

<u>Heat Treatment</u>	<u>Hardness Before Testing (VPN)</u>	<u>Microstructure (figure number)</u>		<u>Rupture Life (hours)</u>	<u>Elonga- tion (percent)</u>	<u>Reduction of Area (percent)</u>
		<u>Before Testing</u>	<u>After Testing</u>			
4 hours at 1975°F, air cooled.	380	3a	8	71.7 48.7	7 15	8 12
2 hours at 2150°F, air cooled.	353	3b	9	147.4 133.7	5 6	5 8
2 hours at 2150°F, air cooled + 4 hours at 1975°F, air cool- ed.	354	3c	-	138.1	4	5

The rupture life for the specimen treated only at 1975°F was considerably less than for the specimens treated at 2150°F, and the difference is considered to indicate a significant difference in properties as shown in the appendix. Conversely, the ductility of the specimen treated only at 1975°F was higher.

It is apparent from the microstructures that heat treatment at 1975°F left a coarse precipitate of  $\gamma'$ . Micrographs of the sample simply treated at 1975°F (no treatment at 2150°F) revealed a grain structure with some non-uniformity of grain size, and a banded distribution of undissolved  $\gamma'$  particles. In addition, the microstructure after testing (see fig. 8) showed the presence of many small areas where overaging occurred during testing. The high hardness of this sample before testing also indicated that residual rolling effects were present. The double treatment at 2150° and 1975°F removed these rolling effects, as evidenced by the lowered hardness, but left residual precipitation (see fig. 3c).

The optical micrographs of figures 3a and 3c indicate two types of banding in these specimens: the narrow banding running generally parallel to the direction of rolling (see fig. 3c) and the broader banding in the specimen treated at

1975°F which runs at an angle to the fine bands (see fig. 3a). These latter bands are thought to be produced by precipitation of larger particles of  $\gamma'$  phase in regions of residual stresses from rolling operations. The finer bands are thought to indicate inhomogeneities in the distribution of the titanium and aluminum in the alloys.

Knowledge of these observations allows one to analyze the stress-rupture results from the study of effect of solution treatment on high-temperature properties. A clearly significant increase in rupture life resulted from including a 2150°F treatment in the heat treatment after rolling. When either the 2150°F, or the 2150°F plus 1975°F treatments were used, the rupture life was significantly higher than when only the 1975°F treatment was used.

It can be postulated that one or both of two causes operated here: (1) incomplete removal of residual working effects from rolling, and/or (2) incomplete solution of  $\gamma'$ . The fact that the 2150° plus 1975°F treatment (with incomplete solution of  $\gamma'$ ) gave essentially the same rupture life as the 2150°F treatment (with complete solution of  $\gamma'$ ) indicates that the second cause was not governing. Then it is apparent that the 1975°F treatment was inferior because it did not completely remove the residual rolling effects. The inhomogeneous structure and high hardness after the solution treatment support this conclusion.

In hot-rolling work on alloys of this type, it has often been found that residual rolling effects are not removed by a 4 hour at 1975°F treatment. Removal of effects from working at 2150°F can require several minutes of reheat time at 2150°F. Evidently, the residual effects alter the aging reaction during subsequent testing and lower rupture life.

#### Effect of Cooling Rate after Solution Treatment

It has been established by Dennison (ref. 10) that cooling rate after solution treatment has a marked influence on subsequent high-temperature properties of

some age-hardening alloys. Specifically, in alloys which were subject to localized grain-boundary precipitate or cellular precipitation, furnace cooling resulted in superior properties in comparison to the faster rates of cooling. To study the effects of cooling rates on the properties of the present alloy, metallographic specimens and rupture specimens were prepared using ice-brine quenching, air cooling and furnace cooling after solution treatment of 2 hours at 2150°F. In addition, one metallographic specimen was water quenched. Figure 10 shows the microstructures and hardnesses of these samples. The electron micrographs show that rapid precipitation of the  $\gamma'$  phase occurred when the alloy was air cooled or furnace cooled but no such precipitation was resolved after water quenching or ice-brine quenching. Neither the optical nor the electron micrographs revealed much localized precipitation at the grain boundaries after any of these treatments.

The relatively high hardness of the air-cooled specimen correlates with the microstructural evidence of a fine dispersion of the  $\gamma'$  particles within the matrix, and the relatively low hardness of the furnace-cooled specimen correlates with the fact that micrographs show a greatly overaged condition of the  $\gamma'$  particles. The fact that the hardness of the water-quenched specimen is slightly greater than that of the ice-brine quenched specimen suggests the occurrence of an extremely fine dispersion of  $\gamma'$  particles which are not resolved by the electron micrographs. Such a fine dispersion may also exist in the ice-brine quenched specimen to account for its hardness of 313 VPN, which is surprisingly high for a fully solutioned alloy of this type.

#### Variation of Stress-Rupture Properties with Cooling Rate after Solution Treatment

To establish the effect of cooling rate on the high-temperature properties, rupture samples were tested at 1600°F and 25,000 psi. The complete specimen treatments and test results, as extracted from table II, were:

<u>Heat Treatment</u>	<u>Hardness Before Testing (VPN)</u>	<u>Microstructure (figure number)</u>		<u>Rupture Life (hours)</u>	<u>Elonga- tion (percent)</u>	<u>Reduction of Area (percent)</u>
		<u>Before Testing</u>	<u>After Testing</u>			
2 hours at 2150°F, ice-brine quenched +4 hours at 1975°F, ice-brine quenched. +24 hours at 1550°F, air cooled +16 hours at 1400°F, air cooled.	402	3d	11	0	<1	<1
2 hours at 2150°F, air cooled +4 hours at 1975°F, air cooled +24 hours at 1550°F, air cooled +16 hours at 1400°F, air cooled.	380	3e	12	152.9	3	6
2 hours at 2150°F, air cooled.	353	3b	9	147.4 133.7	5 6	5 8
2 hours at 2150°F, furnace cooled.	311	3f	13	77.3 69.6	9 6	8 7

Comparison of the first sample above with the second indicates that ice-brine quenching had a very deleterious effect on both rupture life and ductility. Comparison of the third and fourth samples reveals that furnace cooling resulted in significantly lower rupture life than air cooling (see appendix). The slight improvement in ductility after furnace cooling was probably not statistically significant.

In comparing the microstructures of the ice-brine quenched and aged sample with the air-cooled and aged sample after testing (see figs. 11 and 12), one observes differences in both the general precipitation and the localized precipitates at the grain boundaries. The differences in general precipitate size can be attributed to differences in test time which allowed more aging in the air-cooled

sample. The differences in localized precipitates are considered most significant. The air-cooled and double-aged sample exhibited massive  $\gamma'$  particles (from the 1975°F treatment) and some carbides at the grain boundaries while the ice-brine quenched and aged sample had undergone cellular precipitation at some boundaries. It is believed that this cellular precipitate formed during aging prior to loading as a result of residual strains induced at the grain boundaries by the ice-brine quenching, and was related to the brittle, weak characteristics of the ice-brine quenched sample. This is consistent with the conclusions of Roberts (ref. 11) that plastic deformation favored cellular precipitation over general precipitation in Mg-Al alloys due to a build-up of elastic-strain energy at the boundaries, and that the comparatively poor elevated-temperature creep properties accompanied the presence of the cellular precipitation which allowed easy deformation at the grain boundaries. Dennison (ref. 10) also observed that cellular precipitation invariably resulted in low ductilities and low rupture strengths in Cu-Al alloys with additions of Co, Ni and Fe because of rapid, brittle fracture through the grain boundaries.

Air cooling after solution treatment precipitated a finer dispersion of  $\gamma'$  particles than furnace cooling (see fig. 10). Furnace cooling resulted in a coarse general precipitate. The essential feature here is the comparison of the probable precipitate size at the time of rupture-test loading after the four-hour preheat at 1600°F. Microstructures taken of aged specimens in the following study of aging suggest that the air-cooled sample was overaged. Therefore, it is probable that the inferiority of the furnace-cooled condition resulted from the overaging of the  $\gamma'$  precipitate. It is entirely possible that a cooling rate intermediate to air cooling and furnace cooling would improve rupture life over the furnace-cooled condition.

### Effect of Isothermal Aging after Solution Treatment

Studies of the effects of isothermal aging on microstructure and hardness were made with samples aged 1, 10, and 100 hours at 1000°, 1200° and 1400°F and 1, 4, 10 and 100 hours at 1600°F. Two initial conditions were used for each of these aging conditions: solution treatment for 2 hours at 2150°F followed by air cooling; and solution treatment for 2 hours at 2150°F followed by ice-brine quenching. These differed in that considerable precipitation of the  $\gamma'$  phase occurred during air cooling whereas ice-brine quenching gave a more precipitate-free condition prior to aging.

Hardness curves for the aged specimens are plotted in figures 14 and 15. These curves show several interesting general trends in development of hardness which appear to be independent of prior cooling rate:

1. Aging at 1000°F increased hardness little.
2. Hardness increased progressively up to 100 hours at 1200° and 1400°F with no apparent overaging.
3. Overaging occurred at 1600°F after about 4 hours.

In addition, comparison of figure 14 and figure 15 shows several trends which apparently resulted from the differences in the initial treatment before aging:

1. Hardness increased more rapidly at 1200° and 1400°F after ice-brine quenching than after air cooling.
2. The difference in the initial precipitate present in the air-cooled and ice-brine quenched conditions affected the aging curves at 1000° and 1200°F. Longer aging times were needed to reach a given hardness level when the initial condition was ice-brine quenched.
3. At 1400°F, although the hardness after aging 1 hour was lower in the ice-brine quenched sample, longer aging times gave approximately the same hardness level with both starting conditions.

4. During aging at 1600°F, the samples initially ice-brine quenched reached a higher hardness level and resisted overaging to a greater extent.

Representative micrographs of the aged samples are included in figures 16 through 18. It was observed from these that:

1. The general  $\gamma^f$  precipitate was not clearly resolvable by optical microscopy after any of the aging treatments. Aging did develop the precipitate so that evidence of it was seen in optical micrographs as a general greying or spotting of the background. The general  $\gamma^f$  precipitate was resolved by electron microscopy in all samples aged at 1400° and 1600°F.
2. Significant changes occurred in the grain boundaries during aging. In general, the grain boundaries broadened with increasing temperature and time at temperature. Localized precipitation and agglomeration of  $\gamma^f$  at the boundaries was accompanied by precipitation of another phase presumed to be a carbide. The duplex constitution of the boundaries was substantiated by etching techniques illustrated by figures 18c and 18d. This finding is in agreement with that of Baillie and Poulignier (ref. 12). They found evidence for two phases at the grain boundaries of nickel-base alloys with one of the phases evolving and etching like  $\gamma^f$ .
3. A cellular precipitation occurred at the grain boundaries during aging after ice-brine quenching. This localized precipitation was most pronounced at 1200° and 1400°F and preceded general precipitation in the matrix. The particles in the cells appeared like  $\gamma^f$  in electron micrographs.



4. The electron micrographs indicated that the visible general precipitate changed little during aging at 1000° and 1200°F. Aging at 1400° and 1600°F after both initial treatments resulted in growth of the precipitate particles. In considering these overall results it is interesting to note that there is generally a good correlation between the size and distribution of the  $\gamma'$  particles and the hardness of the alloy. The general precipitate in the specimens which were air cooled and subsequently aged 100 hours at 1200° (see fig. 17b) and 1400°F (see fig. 17c) is very similar to that of the specimen which was ice-brine quenched and aged 100 hours at 1400°F (see fig. 16c) and all of these specimens have nearly the same hardness.

#### Variation of Stress-Rupture Properties with Aging Treatment

In order to establish the effect of aging after solution treatment prior to testing on the high-temperature properties, samples were prepared as listed below. When tested at 1600°F and 25,000 psi, the results (from table II) were as tabulated:

<u>Heat Treatment</u>	<u>Hardness Before Testing (VPN)</u>	<u>Microstructure (figure number)</u> <u>Before</u> <u>After</u> <u>Testing</u> <u>Testing</u>		<u>Rupture Life (hours)</u>	<u>Elonga- tion (percent)</u>	<u>Reduction of Area (percent)</u>
2 hours at 2150°F, air cooled +24 hours at 1550°F, air cooled +16 hours at 1400°F, air cooled.	389	3g	--	127.6	5	3
2 hours at 2150°F, air cooled.	353	3b	9	147.4 133.7	5 6	5 8
2 hours at 2150°F, air cooled +4 hours at 1975°F, air cooled +24 hours at 1550°F, air cooled +16 hours at 1400°F, air cooled.	380	3e	12	152.9	3	6

<u>Heat Treatment</u>	<u>Hardness Before Testing (VPN)</u>	<u>Microstructure (figure number)</u>		<u>Rupture Life (hours)</u>	<u>Elonga- tion (percent)</u>	<u>Reduction of Area (percent)</u>
		<u>Before Testing</u>	<u>After Testing</u>			
2 hours at 2150°F, air cooled +4 hours at 1975°F, air cooled.	354	3c	--	138.1	4	5

Comparison of the first sample with the second and of the third with the fourth sample shows that no significant effect of aging prior to testing was found (see appendix). The microstructures before testing show that all the samples had a fine dispersion of  $\gamma^f$  before testing.

It is probable that the four-hour preheat time at 1600°F before stressing acted as an equalizer. All the samples were probably aged to near maximum hardness and optimum precipitate dispersion, thereby masking the effect of prior aging.

Although the data showed that solution treatment at 2150°F followed by air cooling gave rupture life comparable to an aged specimen, the results might have differed somewhat if different rupture-testing conditions and preheat time had been used. However, it suffices to state that the optimum rupture life will probably be obtained with a pre-treatment which avoids grain boundary overaging before testing and gives a dispersion of  $\gamma^f$  aged near maximum hardness at the time of loading.

#### Cellular Precipitation

A high incidence of cellular precipitation was observed at the grain boundaries of specimens aged after ice-brine quenching from the solution treatment whereas the general tendency in specimens which were not ice-brine quenched was for a more uniform agglomeration of the  $\gamma^f$  and carbide phases. The development of the cellular precipitate in the grain boundaries was very rapid, and in the specimens aged at 1200°F preceded visible evidence of general precipitation of the  $\gamma^f$  (see fig. 16b).

In many cases, the cellular particles seemed to nucleate at points in the matrix near the grain boundaries (see figs. 16b and 16c) and then grow. The size of the  $\gamma'$  particles in the cells was usually large compared to that in the adjoining matrix, and the general condition within the cells appeared to be one of extreme overaging such that there was considerable precipitate-free matrix between the cellular particles.

It seems very possible that the driving force behind this accelerated cellular precipitation near the grain boundaries was thermal stressing. It is known that alloys of this type undergo plastic flow during quenching (ref. 13) resulting in residual strain energy. It is possible that the matrix material near the grain boundaries retained this strain energy after ice-brine quenching, and that this residual strain energy was sufficient to initiate the cellular precipitation during subsequent aging treatments.

#### Effect of Rupture Testing on Structures

The hardnesses of ruptured samples except for the ice-brine quenched and furnace-cooled samples were essentially equal despite the differences in rupture time. They all were in the range of 362 to 368 VPN. This level was significantly higher than the hardness of 328 VPN for the sample aged 100 hours at 1600°F with no stress applied. The microstructures revealed that the general precipitate size and distribution in the matrix corresponded roughly to that of samples aged without stress for a time corresponding to the rupture time. Therefore, stressing seemingly had no effect on the general precipitate size. However, stressing did prevent the hardness decrease which accompanied the overaging in the non-stressed aging samples. Evidently, an increment of hardness was added by the creep deformation which occurred during the rupture test.

The most striking difference between aged specimens and stressed-aged specimens was at the grain boundaries. While part of the grain boundaries of the ruptured specimens closely resembled grain boundaries of aged specimens, the remainder were heavily overaged with large agglomerated particles of  $\gamma'$  in fields of matrix which were otherwise precipitate free. These observations are in agreement with those of Baillie and Poulignier (ref. 12) who found for similar nickel-base alloys that stress had little if any effect on general precipitation during aging but produced some changes at the grain boundaries.

## DISCUSSION

One of the important contributions of this report is to show the microstructures developed in a typical nickel-base alloy under a variety of different heat treatments. The most striking microstructural characteristic of this type of alloy is the large amount of the intermetallic  $\gamma'$  phase which precipitates within the matrix grains and the rapidity with which it forms. For the 55 Ni - 20 Cr - 15 Co - 4 Mo - 3 Ti - 3 Al alloy studied here, the temperature for complete solution of this phase was found to be between 1975° and 2000°F, and very rapid cooling by water or ice-brine quenching was required after solution treatment to prevent re-precipitation of resolvable amounts of  $\gamma'$  phase. Short periods of aging of 1400° to 1600°F or air cooling after solution treatment produce a very close dispersion of  $\gamma'$  particles which are only a few hundred angstrom units in diameter. Additional aging at these temperatures causes an increase in both the size and the separation of these particles. Aging at temperatures of 1200°F and below for periods of as much as 100 hours appears to have little effect on the precipitation of the  $\gamma'$  phase, while aging for only a few hours at temperatures of 1700° to 1900°F produces severe overaging

characterized by very large and widely separated particles. In all cases, except with furnace cooling after solution treatment, these  $\gamma'$  particles appeared spheroidal in shape. It was particularly interesting that microstructures produced by aging under stress were very similar to those produced by comparable aging treatments without stress.

Precipitation at the grain boundaries consisted of two phases; one apparently a carbide phase and the other the  $\gamma'$  phase. Aging after air cooling from solution treatment generally appeared to result in a gradual development of these phases at the grain boundaries, with no particular evidence of depletion of the nearby matrix areas. This process was generally slow compared to the development of a cellular type of precipitation at a large fraction of the grain boundaries during aging after ice-brine quenching. This appeared to consist of rods or plates of the  $\gamma'$  phase extending outward from the grain boundaries and surrounded by depleted regions of matrix. The development of this condition was rapid compared to the matrix precipitation; aging 100 hours at 1200°F after ice-brine quenching from solution treatment produced extensive cellular precipitation but no detectable  $\gamma'$  particles in the matrix.

The observation of these microstructural characteristics required the use of both optical and electron microscopy. The presence and extent of the cellular precipitation could be observed most readily in optical micrographs of 100 or 1000 D, and the existence of overaged  $\gamma'$  particles in the matrix could generally be deduced from the general darkening of the matrix in these micrographs. For the observation of the fine details of the size, shape, and distribution of the  $\gamma'$  particles and of the structure of the cellular precipitate, however, electron microscopy was required. Methods of preparing alloy specimens for observation by electron and optical microscopy have been described.

Attempts have been made to relate the observed microstructure to the hardness of the alloy and its stress-rupture properties measured at 1600°F and 25,000 psi. Hardness generally appeared to be most closely related to the distribution of the  $\gamma'$  particles within the matrix of the alloy: a fine dispersion of small particles was usually accompanied by high hardness while the overaged structures involving the large, widely-separated particles were associated with lower hardness. The microstructural observations are not completely effective in correlating all observed variations in hardness, however. The fact that aging specimens at 1000° and 1200°F after solution treatment at 2150°F and ice-brine quenching produced increases in hardness without producing detectable  $\gamma'$  particles is a case in point. It may be that here  $\gamma'$  particles were produced which were too fine to be resolved by the etching and replicating techniques used in obtaining the electron micrographs. A similar explanation may account for the fact that the alloy did not soften as much as might be expected upon solution treatment at 2000°F and ice-brine quenching, and that its hardness after this treatment was higher than after solution treatment at 1900°F and ice-brine quenching. In this case, however, solution hardening due to more complete dissolving of the elements forming the  $\gamma'$  phase may be involved.

The stress-rupture properties of the alloy appear to be more closely related to the conditions of the grain boundaries than to the general precipitation of the  $\gamma'$  phase within the matrix. It appears that overaged conditions at the grain boundary regions are associated with weakness in the 1600°F rupture tests. These conditions can develop from aging during testing or from treatments prior to the start of a rupture test, as was the case for ice-brine quenching or furnace cooling after solution treatment. Material treated only at 1975°F was more prone to the development of this type of structure during testing than material heated at 2150°F, apparently because the higher temperature is more effective in removing residual

rolling effects. It is highly possible that the weakness and overaged grain boundary structures are due to strain-induced phenomena arising from quenching stresses, residual cold work from rolling and, in rupture testing, from yielding and creep.

Since the alloy seemed to be strain sensitive, the influence of rolling when solution treatments are carried out at about 1975°F would be expected to be variable. If the rolling gave uniform complete recrystallization, it might have considerably less effect. Likewise, if it left enough residual strain to give uniform recrystallization on heating to 1975°F it ought to have little effect. The restrictions imposed by the limited range of temperatures and reduction of hot rolling needed to minimize cracking, however, suggest that this alloy should usually be improved by a higher temperature treatment. It is strongly suspected that the alloy is subject to considerable loss in strength at 1600°F from small amounts of cold work. Because the alloy apparently cold works to a considerable extent during working at temperatures as high as 2150°F, and since considerable time is needed to anneal the alloy even at 2150°F, the chances are that there are only rare cases where the 2150°F treatment would not be beneficial.

In conclusion, it is known that very small amounts of such elements as boron, zirconium and possibly magnesium have very pronounced effects on strength and ductility in rupture tests (ref. 14). Work is in progress to determine how the presence of traces of such elements affect the microstructures and properties of this and similar alloys. Until such studies are complete and further verification of the relationships are obtained experimentally, it cannot be estimated to what extent the results described here can be extrapolated to other alloys and other conditions of heat treatment and testing. However, it can be noted that general trends in the variations of hardness and stress-rupture properties with heat treatment described for the experimental alloy used here are similar to those which have been observed in limited studies of other experimental alloys of similar compositions.

## CONCLUSIONS

The study of effects of heat treatments on microstructures and high-temperature properties of a Ti + Al hardened nickel-base alloy resulted in several conclusions.

The solution temperature for complete solution of  $\gamma^f$  and grain boundary carbides during a 4-hour heat treatment was between 1975° and 2000°F.

Heat treatment at 1800° to 1900°F led to overaging of the alloy. The coarse general precipitate of  $\gamma^f$  was obtained in this range and resulted in significantly lower hardness than in the completely solutioned and quenched condition.

The rupture life of stock solution-treated 4 hours at 1975°F and air cooled was inferior to that treated 2 hours at 2150°F, air cooled. This was related to residual rolling effects which were not removed by the 1975°F treatment.

Cooling rate after solution treatment markedly affected the precipitation reaction during the cooling period and during subsequent aging. Rapid general precipitation of  $\gamma^f$  occurred during cooling. Considerable suppression of the reaction was obtained by ice-brine quenching although it was not proved that suppression was complete. Precipitation increased inversely with cooling rate, with air cooling giving a general fine precipitate but furnace cooling a coarse overaged general precipitate. Aging of the ice-brine quenched stock led to cellular precipitation at the grain boundaries.

Cooling rate after solution treatment also had a marked effect on high-temperature properties. Solution treated, ice-brine quenched and aged stock ruptured upon loading at 1600°F and 25,000 psi with negligible ductility. This was related to the cellular precipitate. Furnace cooling after solution treatment resulted in inferior rupture life in comparison to air cooling, because the furnace-cooled sample was overaged before testing.



Isothermal-aging studies revealed that general precipitation of  $\gamma'$  proceeded at 1200°, 1400° and 1600°F. Localized precipitation of  $\gamma'$  and carbides appeared at grain boundaries at 1400° and 1600°F. No overaging was evident during 100 hours at 1200° and 1400°F; but overaging did occur after 4 hours at 1600°F. No significant effect of the double-aging treatment after solution treating and air cooling on rupture life was found.

Comparison of samples rupture tested at 1600°F with those aged at 1600°F without stress revealed that stress had little effect on the precipitation of the  $\gamma'$  particles within the alloy matrix. Stressing did appear to cause severe agglomeration and overaging to a greater extent at the grain boundaries. In addition, stressing prevented the drop-off of hardness that accompanied overaging of the matrix precipitate in the isothermally-aged unstressed samples.

It is concluded that effects of heat treatments on the high-temperature properties of the Ti + Al hardened nickel-base alloy were related to the  $\gamma'$  size and distribution as follows:

1. Treatments which provided a finely dispersed general precipitate of  $\gamma'$  with no overaged areas of depleted matrix resulted in essentially equal properties at 1600°F and 25,000 psi.
2. Treatments such as ice-brine quenching or furnace cooling which resulted in overaging of portions of the stock (the cellular precipitate in the case of ice-brine quenching and the general precipitate in the case of furnace cooling ) lowered the high-temperature life.

## REFERENCES

1. Nordheim, R., Grant, N. J. "Aging Characteristics of Nickel-Chromium Alloys Hardened with Titanium and Aluminum." Journal of Metals, Vol. 6, Feb. 1954, p. 211.
2. Taylor, A. "Constitution of Nickel-Rich Quaternary Alloys of the Ni - Cr - Ti - Al System." Journal of Metals, Vol. 8, Oct. 1956, p. 1356.
3. Betteridge, W., Franklin, A. W. "Les Progrès des Alliages à Base de Nickel-Chrome en Service à Haute Temperature." Revue de Metallurgie, Vol. 53, April 1956, p. 271.
4. Freeman, J. W., Corey, C. L. "Microstructure and Creep," Creep and Fracture of Metals at High Temperatures. Her Majesty's Stationery Office, London, 1956.
5. Frey, D. N., Freeman, J. W., White, A. E. "Fundamental Aging Effects Influencing High-Temperature Properties of Solution-Treated Inconel X." NACA TN 2385, 1951.
6. Brockway, L. O., Bigelow, W. C. "The Investigation of the Minor Phases of Heat-Resistant Alloys by Electron Diffraction and Electron Microscopy." WADC Technical Report 54-589, Wright Air Development Center, Wright-Patterson Air Force Base, Ohio, May 1955.
7. Betteridge, W., Smith, R. A. "Effect of Heat Treatment and Structure upon Creep Properties of Nimonic Alloys Between 750 and 950°C." Symposium on Metallic Materials for Service at Temperatures above 1600°F. ASTM, Philadelphia 3, Pa., 1956.
8. Geisler, A. H. "Precipitation from Solid Solutions of Metals," Phase Transformations in Solids. John Wiley and Sons, Inc., New York, 1951.
9. Bigelow, W. C., Amy, J. A., Brockway, L. O. "A Selective Etching Procedure for Identifying the  $\gamma'$  Phase of Nickel-Base Alloys by Electron Microscopy." Paper presented at ASTM annual meeting, 1955. To be published.
10. Dennison, J. P. "Some Creep Characteristics of a Group of Precipitation-Hardening Alloys Based on the Alpha-Copper-Aluminum Phase." Journal of Institute of Metals, Vol. 82, November 1953, p. 1504.
11. Roberts, C. S. "Interaction of Precipitation and Creep in Mg-Al Alloys." Journal of Metals, Vol. 8, Feb. 1956, p. 146.

12. Baillie, Y., Poulignier, J. "La Précipitation Submicroscopique dans les Alliages Refractaires Nickel-Chrome." Revue de Metallurgie, Vol. 51, March 1954, p. 179.
13. Decker, R. F., Rush, A. I., Dano, A. G., Freeman, J. W. "Abnormal Grain Growth in Nickel-Base Heat-Resistant Alloys." Engineering Research Institute, University of Michigan, Report 51 to The National Advisory Committee for Aeronautics, May 11, 1956.
14. Decker, R. F., Rowe, J. P., Freeman, J. W. "Influence of Crucible Materials on the High-Temperature Properties of a Vacuum-Melted 55 Ni - 20 Cr - 15 Co - 4 Mo - 3 Ti - 3 Al Alloy." Engineering Research Institute, University of Michigan, Report 55 to The National Advisory Committee for Aeronautics, January 18, 1957.
15. Duncan, A. J. Quality Control and Industrial Statistics. Richard D. Irwin, Inc. Homewood, Illinois, 1952.

TABLE I  
ETCHANTS USED IN METALLOGRAPHIC STUDY

<u>Designation</u>	<u>Composition</u>	<u>Percent by Volume</u>
<u>Designation</u>	<u>Component</u>	<u>Percent by Volume</u>
Etchant A	Cupric chloride solution <sup>(1)</sup>	29
	Acetic acid (glacial)	36
	Hydrochloric acid (38%)	23
	Sulfuric acid (96%)	5
	Chromic acid <sup>(2)</sup>	7
Etchant B	Phosphoric acid (85%)	12
	Sulphuric acid (96%)	47
	Nitric acid (70%)	41
Etchant C	Phosphoric acid (85%)	11
	Sulphuric acid (96%)	45
	Nitric acid (70%)	29
	Water	15
Etchant D	Sulphuric acid (96%)	21
	Hydrochloric acid (38%)	15
	Nitric acid (70%)	21
	Hydrofluoric acid (48%)	21
	Water	22
Etchant E	Cupric chloride solution <sup>(1)</sup>	40
	Hydrochloric acid (38%)	40
	Hydrofluoric acid (48%)	20

(1) Solution of 1 gram  $\text{CuCl}_2 \cdot 2\text{H}_2\text{O}$  per 5 ml.  $\text{H}_2\text{O}$

(2) Solution of 1 gram  $\text{CrO}_3$  per 3 ml.  $\text{H}_2\text{O}$

TABLE II  
STRESS-RUPTURE DATA AT 1600°F AND 25,000 PSI

Solution Treatment		Aging Treatment		Rupture Time (hr)	Elongation (percent)	Reduction of Area (percent)	Hardness after Test (VFN)			
Time (hr)	Temperature (°F)	Time (hr)	Temperature (°F)							
4	1975	Air	--	71.7 48.7	7 15	8 12	368			
2	2150	Air	--	147.4 133.7	5 6	5 8	365			
2 +4	2150 1975	Air Air	--	138.1	4	5	362			
2 +4	2150 1975	Ice brine Ice brine	24 +16	1550 1400	1550 1400	Air Air	Broke on loading	<1	<1	402
2 +4	2150 1975	Air Air	24 +16	1550 1400	1550 1400	Air Air	152.9	3	6	362
2	2150	Furnace	--	--	--	--	77.3 69.6	9 6	8 7	325
2	2150	Air	24 +16	1550 1400	1550 1400	Air Air	127.6	5	3	362

TABLE III  
HARDNESS DATA

Vickers Penetration Hardness (50,000 gram load)

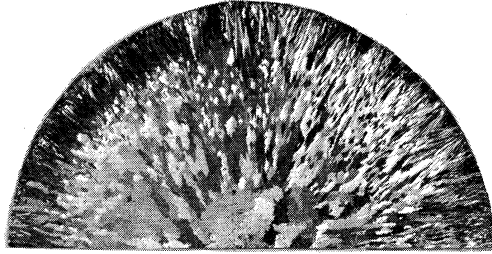
Original Condition	Solution Treatment			Aging Treatment			Hardness (VPN)
	Time (hr)	Temperature (°F)	Cooling Medium	Time (hr)	Temperature (°F)	Cooling Medium	
As Cast (Ingot center)	--	--	--	--	--	--	335
As Cast (Ingot surface)	--	--	--	--	--	--	325
As rolled	--	--	--	--	--	--	362
As rolled	4	1975	Air	--	--	--	380
As rolled	2	2150	Air	--	--	--	356, 354, 349
As rolled	2	2150	Furnace	--	--	--	311
As rolled	2	2150	Air	--	--	--	354
	+4	1975	Air				
As rolled	2	2150	Air	24	1550	Air	380
	+4	1975	Air	+16	1400	Air	
As rolled	2	2150	Ice-brine	24	1550	Air	402
	+4	1975	Ice-brine	+16	1400	Air	
As rolled	2	2150	Air	24	1550	Air	389
				+16	1400	Air	
As rolled	2	2150	Air	4	1700	Ice-brine	348
As rolled	2	2150	Air	4	1800	Ice-brine	298
As rolled	2	2150	Air	4	1900	Ice-brine	276
As rolled	2	2150	Air	4	2000	Ice-brine	306
As rolled	2	2150	Ice-brine	--	--	--	313
As rolled	2	2150	Water	--	--	--	324
As rolled	2	2150	Ice-brine	1	1000	Air	333
As rolled	2	2150	Ice-brine	10	1000	Air	328
As rolled	2	2150	Ice-brine	100	1000	Air	340
As rolled	2	2150	Ice-brine	1	1200	Air	345
As rolled	2	2150	Ice-brine	10	1200	Air	357
As rolled	2	2150	Ice-brine	100	1200	Air	374
As rolled	2	2150	Ice-brine	1	1400	Air	345
As rolled	2	2150	Ice-brine	10	1400	Air	380
As rolled	2	2150	Ice-brine	100	1400	Air	398
As rolled	2	2150	Ice-brine	1	1600	Air	365
As rolled	2	2150	Ice-brine	4	1600	Air	389
As rolled	2	2150	Ice-brine	10	1600	Air	365
As rolled	2	2150	Ice-brine	100	1600	Air	345
As rolled	2	2150	Air	1	1000	Air	345
As rolled	2	2150	Air	10	1000	Air	357
As rolled	2	2150	Air	100	1000	Air	362
As rolled	2	2150	Air	1	1200	Air	359
As rolled	2	2150	Air	10	1200	Air	368
As rolled	2	2150	Air	100	1200	Air	383
As rolled	2	2150	Air	1	1400	Air	377
As rolled	2	2150	Air	10	1400	Air	383
As rolled	2	2150	Air	100	1400	Air	392
As rolled	2	2150	Air	1	1600	Air	359
As rolled	2	2150	Air	4	1600	Air	374
As rolled	2	2150	Air	10	1600	Air	354
As rolled	2	2150	Air	100	1600	Air	328

TABLE IV

## X-RAY DIFFRACTION DATA

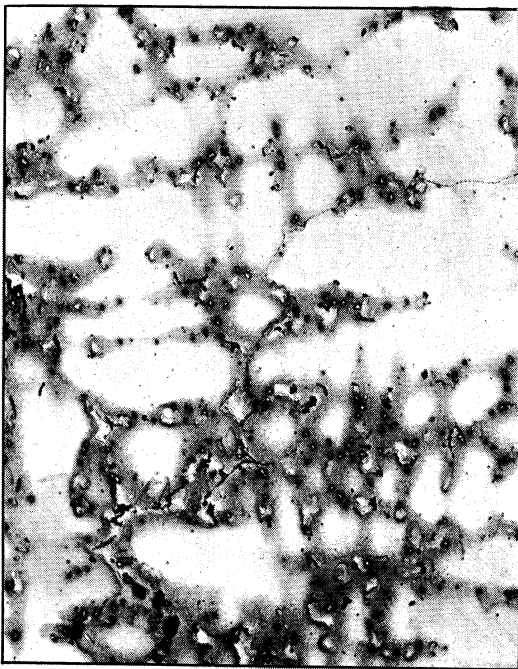
Solid Samples with Unfiltered Cr-K Radiation

4 hours at 1900°F, ice-brine quenched				4 hours at 2000°F, ice-brine quenched		
d	Estimated Intensity	Possible Phase	hkl	d	Estimated Intensity	Possible Phase
3.56	weak very weak	$\gamma'$ $\gamma'$	100 $\alpha$ 100 $\beta$			
2.52	weak	$\gamma'$	110 $\alpha$			
2.06	very strong strong	$\gamma$ $\gamma$	111 $\alpha$ 111 $\beta$	2.07	very strong strong	$\gamma$ $\gamma$
1.79	very strong strong	$\gamma$ $\gamma$	200 $\alpha$ 200 $\beta$	1.79	very strong strong	$\gamma$ $\gamma$
1.27	very strong strong	$\gamma$ $\gamma$	220 $\alpha$ 220 $\beta$	1.27	very strong medium	$\gamma$ $\gamma$
1.19	very weak	$\gamma'$	300 $\alpha$			
1.08	strong	$\gamma$	311 $\beta$	1.08	strong	$\gamma$



Actual Size

(a) As-cast macrostructure of ingot section.



X100D



X1000D

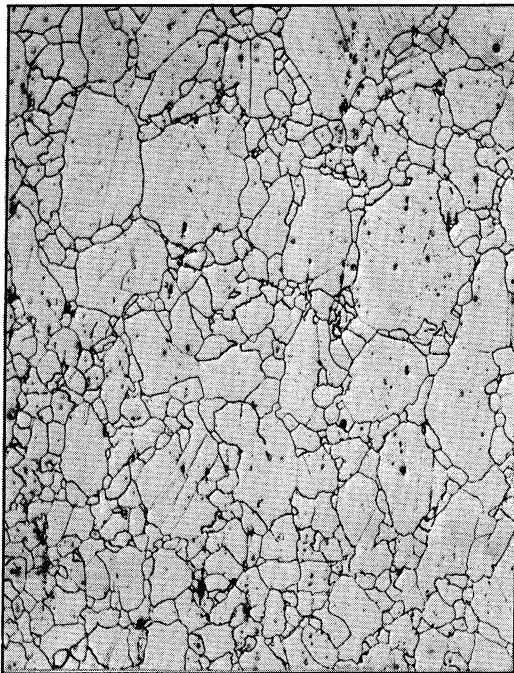
(b) As-cast microstructure at ingot center.

Figure 1. - As-cast structure of experimental alloy.





(a) As-rolled 7/8-inch bar stock.



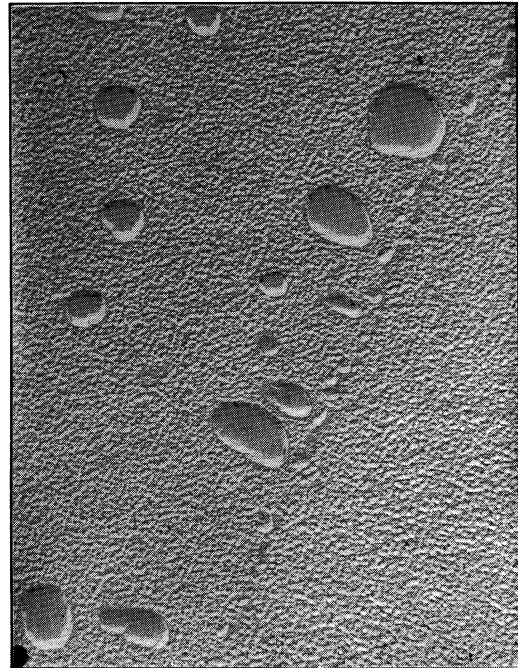
X100D

(b) As-rolled microstructure.

Figure 2. - As-rolled experimental alloy.

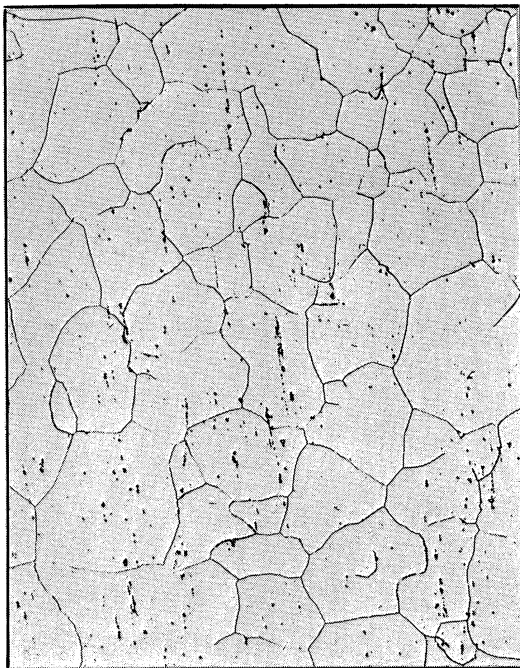


X100D

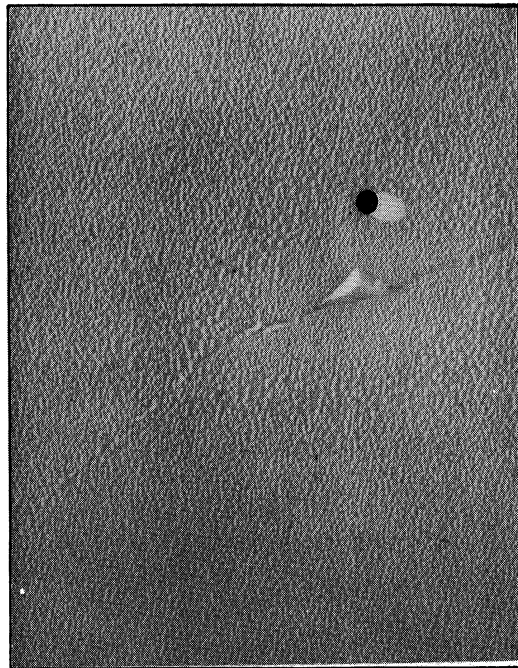


X13,000D

(a) Treated 4 hours at 1975°F, air cooled. Hardness-380 VPN; average rupture life - 60 hours.



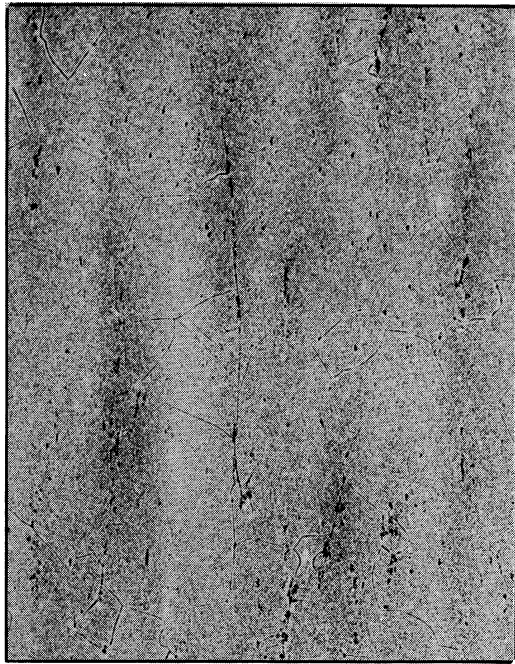
X100D



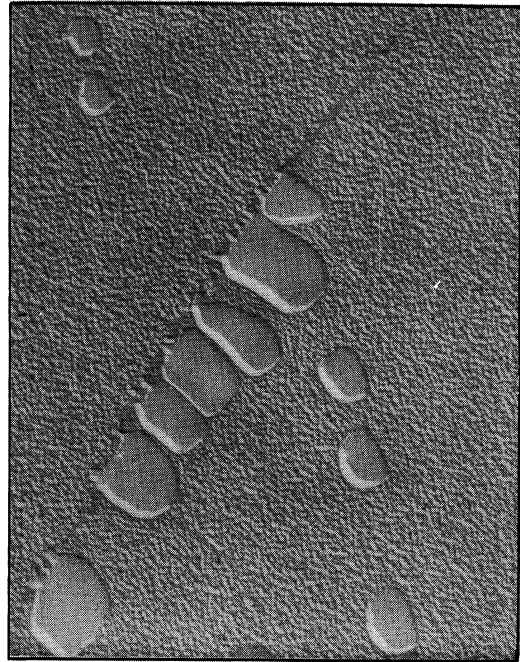
X13,000D

(b) Treated 2 hours at 2150°F, air cooled. Hardness-353 VPN; average rupture life - 140 hours.

Figure 3. - Microstructures of alloy after heat treatment prior to rupture testing. Micrographs at 100D are optical micrographs, those at 13,000D are electron micrographs. Rupture life is given for tests at 1600°F and 25,000 psi.

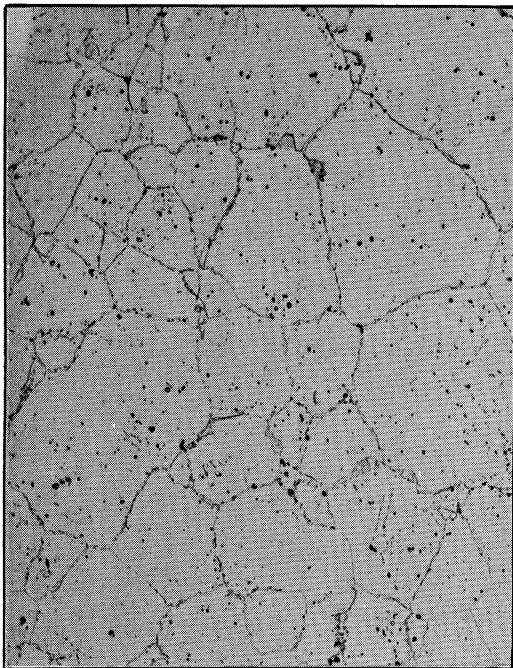


X100D

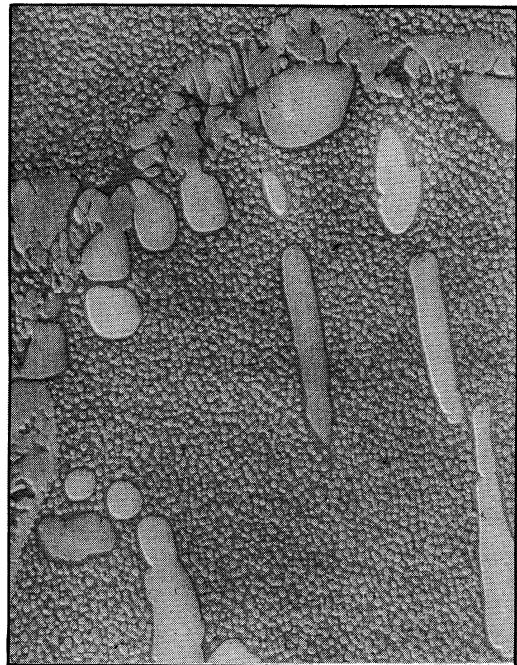


X13,000D

(c) Treated 2 hours at 2150°F, air cooled; plus 4 hours at 1975°F, air cooled. Hardness - 354 VPN; rupture life - 138.1 hours.



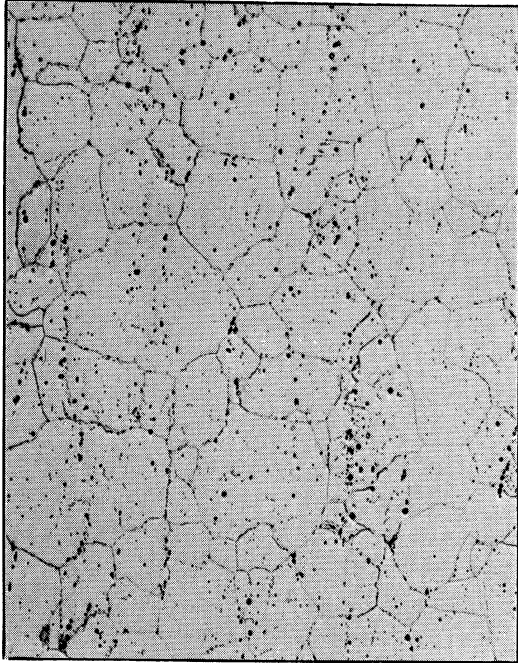
X100D



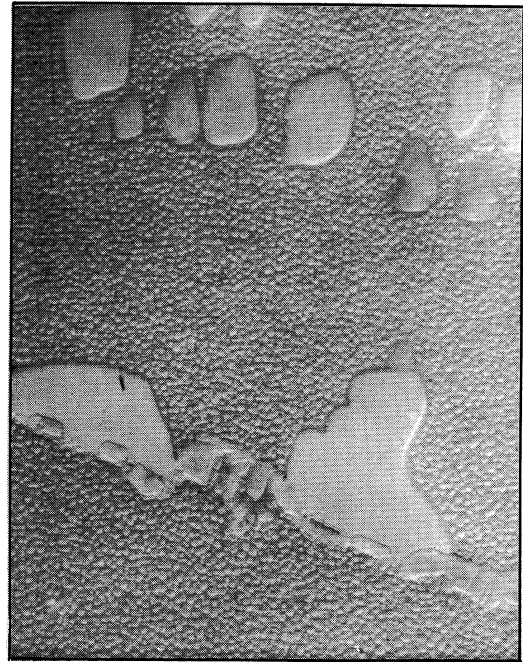
X13,000D

(d) Treated 2 hours at 2150°F, ice-brine quenched; plus 4 hours at 1975°F, ice-brine quenched; plus 24 hours at 1550°F, air cooled; plus 16 hours at 1400°F, air cooled. Hardness - 402 VPN; rupture life - broke on loading.

Figure 3. - Continued.

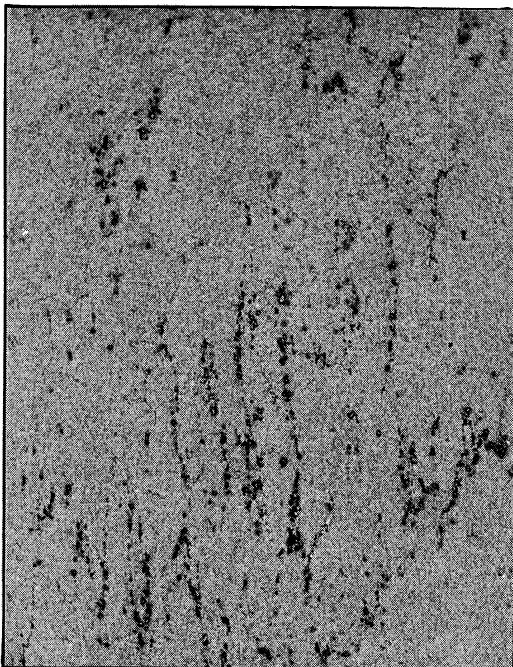


X100D

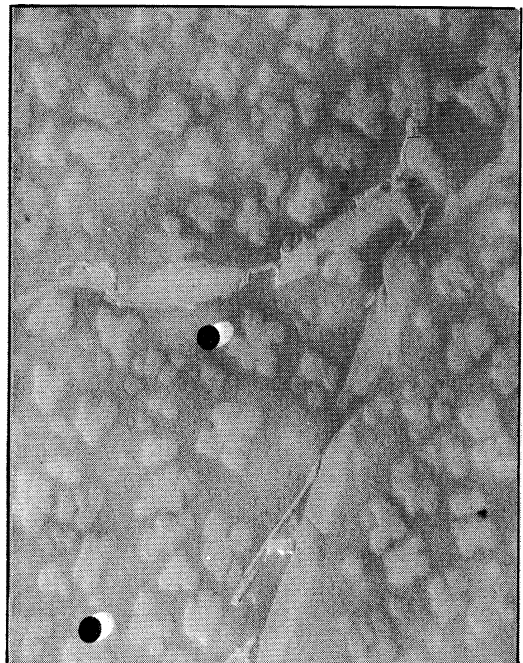


X13,000D

(e) Treated 2 hours at 2150°F, air cooled; plus 4 hours at 1975°F, air cooled; plus 24 hours at 1550°F, air cooled; plus 16 hours at 1400°F, air cooled. Hardness-380 VPN; rupture life - 152.9 hours.



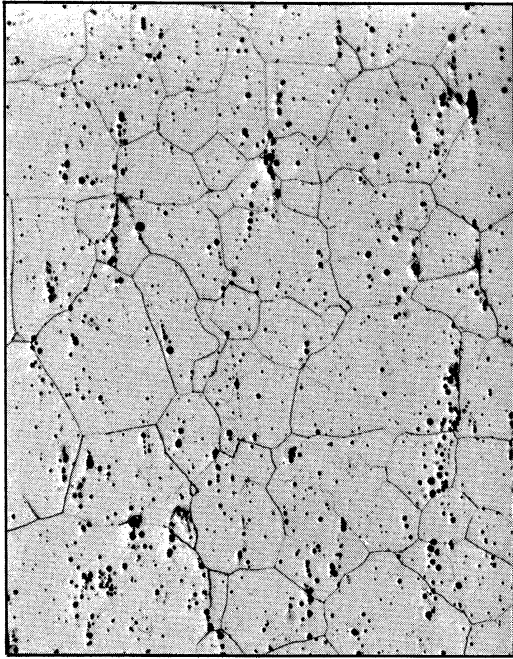
X100D



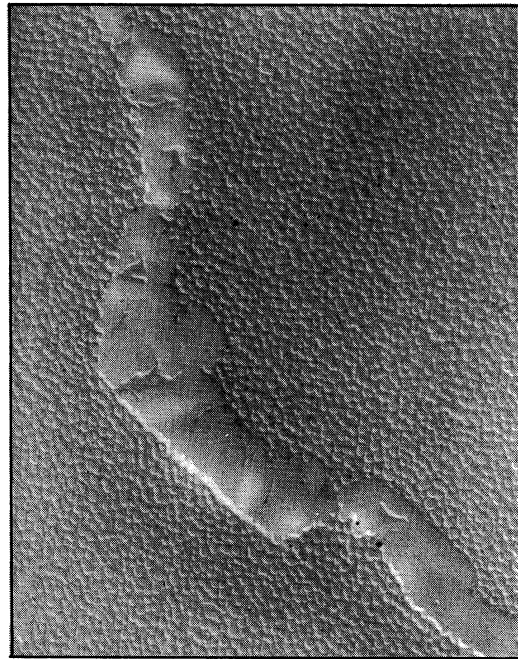
X13,000D

(f) Treated 2 hours at 2150°F, furnace cooled. Hardness-311 VPN; average rupture life - 73 hours.

Figure 3. - Continued.



X100D



X13,000D

(g) Treated 2 hours at 2150°F, air cooled; plus 24 hours at 1550°F, air cooled; plus 16 hours at 1400°F, air cooled. Hardness-389 VPN; rupture life - 127.6 hours.

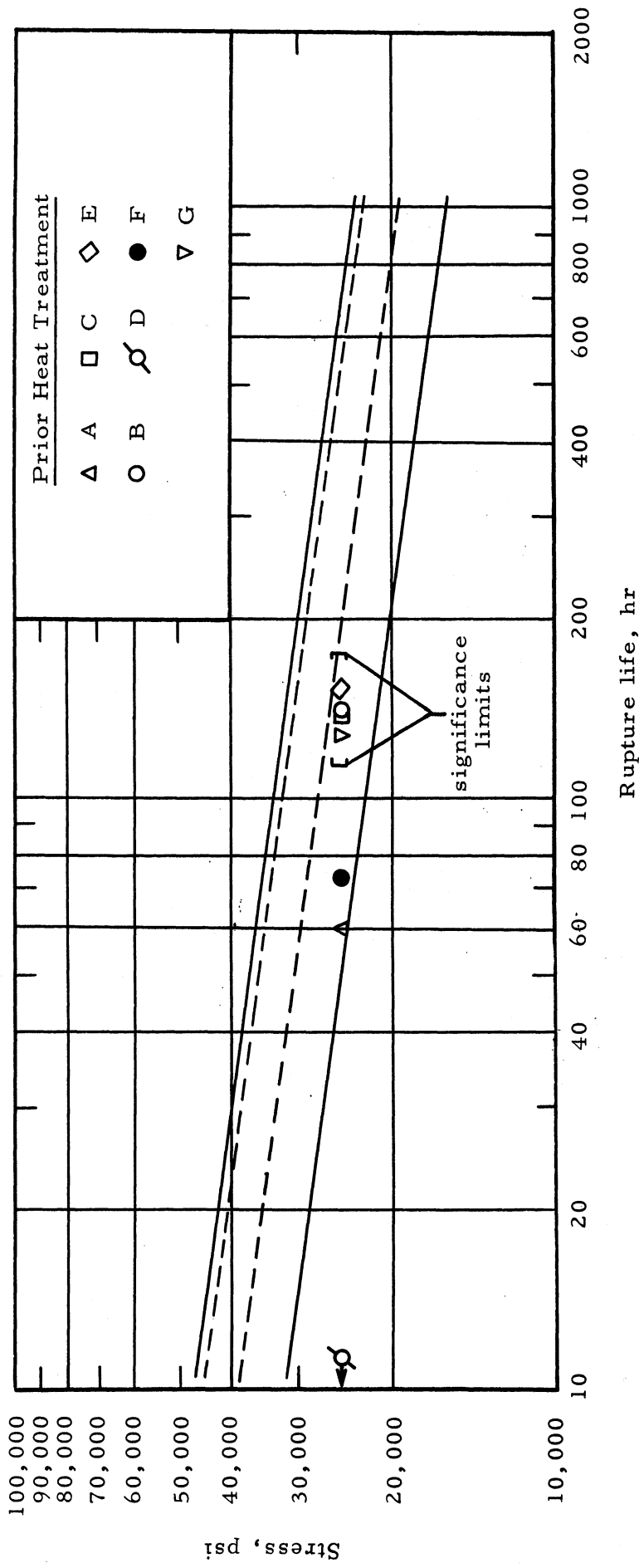
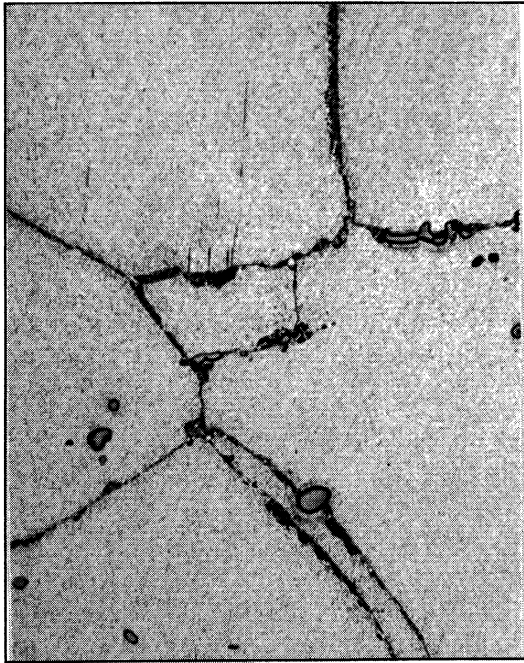
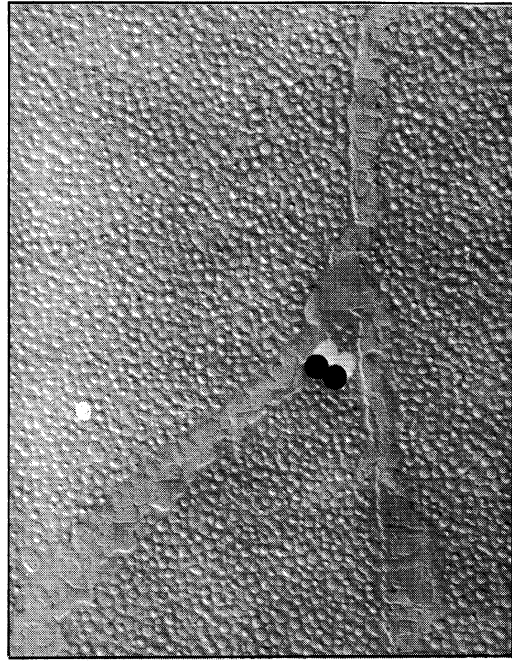


Figure 4. - Variation in rupture life at 1600°F and 25,000 psi with prior heat treatment. Results are plotted on stress-rupture band for 55 Ni - 20 Cr - 15 Co - 4 Mo - 3 Ti - 3 Al alloys. Dashed band based on data on two heats of vacuum-melted Udimet 500 with treatment E reported by Utica Drop Forge and Tool Company. Solid band is extrapolated from data on vacuum-melted heats processed at University of Michigan in study of effect of melting practice and chemistry on rupture life (all heats with treatment B)(ref. 14). See appendix for meaning of significance limits.

- Treatment A - 4 hours at 1975°F, air cooled.
- Treatment B - 2 hours at 2150°F, air cooled.
- Treatment C - 2 hours at 2150°F, air cooled  
+ 4 hours at 1975°F, air cooled.
- Treatment D - 2 hours at 2150°F, ice-brine quenched  
+ 4 hours at 1975°F, ice-brine quenched  
+ 24 hours at 1550°F, air cooled  
+ 16 hours at 1400°F, air cooled.
- Treatment E - 2 hours at 2150°F, air cooled  
+ 4 hours at 1975°F, air cooled  
+ 24 hours at 1550°F, air cooled  
+ 16 hours at 1400°F, air cooled.
- Treatment F - 2 hours at 2150°F, furnace cooled.
- Treatment G - 2 hours at 2150°F, air cooled  
+ 24 hours at 1550°F, air cooled  
+ 16 hours at 1400°F, air cooled.

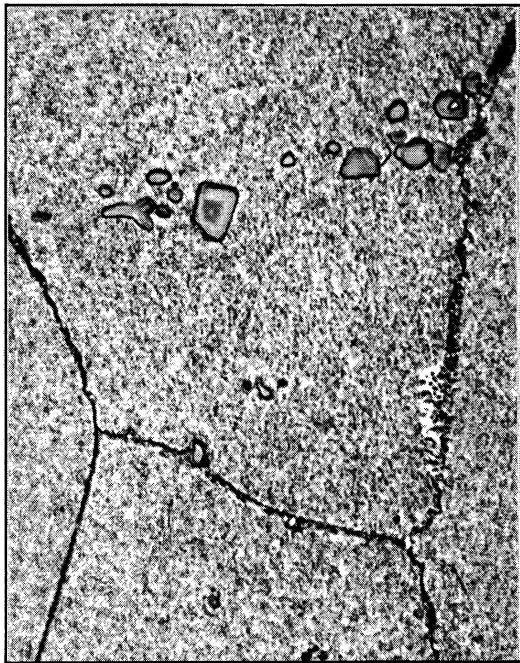


X1000D

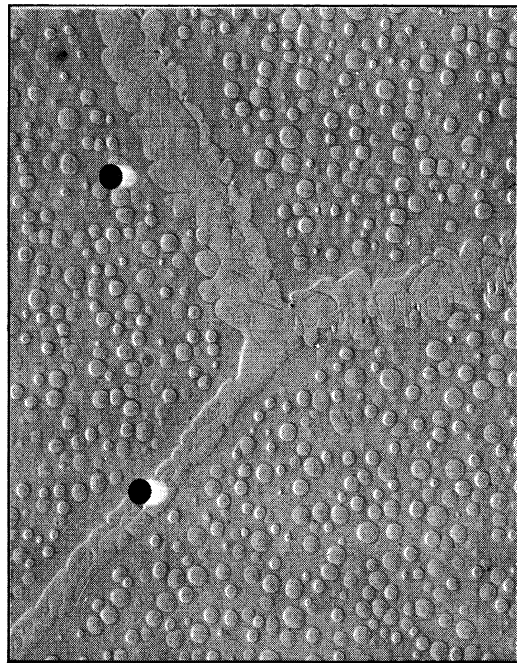


X13,000D

(a) 1700°F, ice-brine quenched; hardness - 348 VPN.



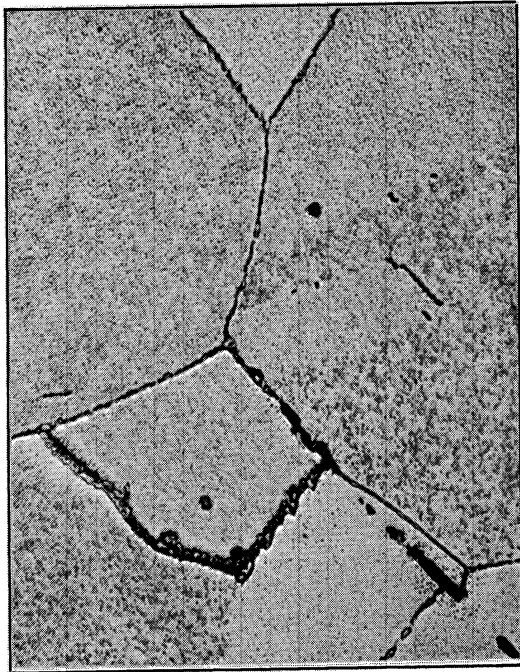
X1000D



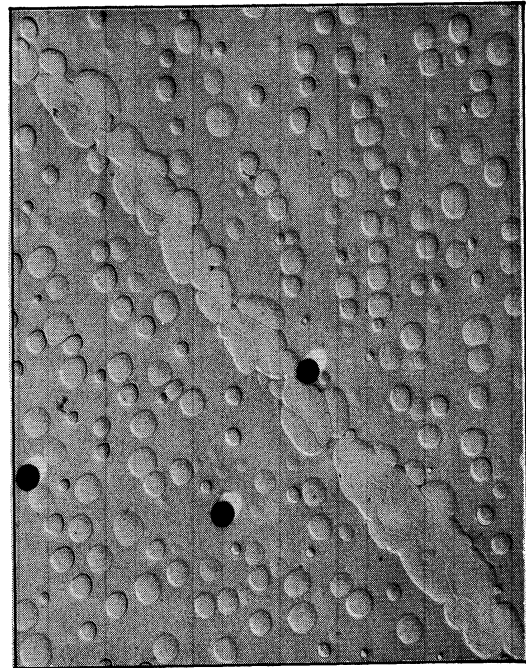
X13,000D

(b) 1800°F, ice-brine quenched; hardness - 298 VPN.

Figure 5. - Effect of 4-hour heat treatments at designated temperatures on microstructure. Rolled bar stock was treated 2 hours at 2150°F, air cooled prior to heat treatment. Micrographs at 1000D are optical micrographs; those at 13,000D are electron micrographs.

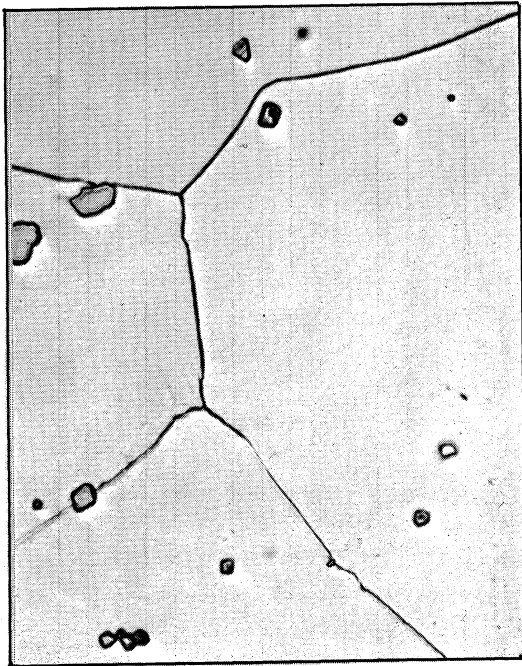


X1000D

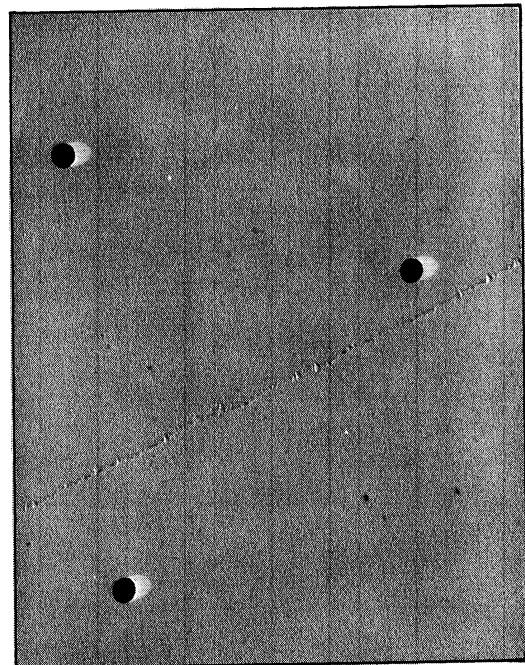


X13,000D

(c) 1900°F, ice-brine quenched; hardness - 276 VPN.



X1000D



X13,000D

(d) 2000°F, ice-brine quenched; hardness - 306 VPN.

Figure 5.- Concluded.



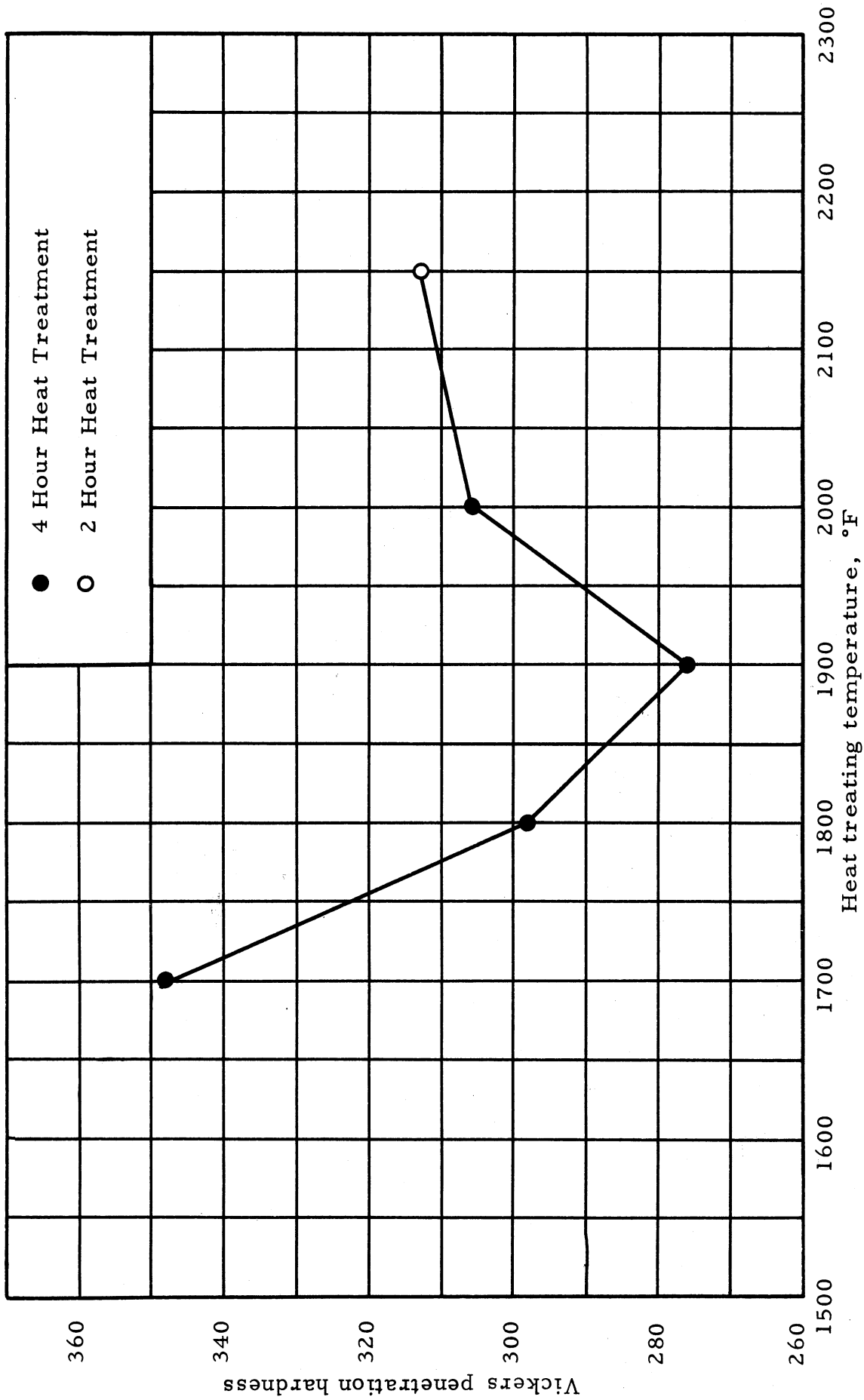


Figure 6. - Effect of heat-treating temperature on hardness. Rolled bar stock was treated 2 hours at 2150°F, air cooled prior to heat treatment. Samples were ice-brine quenched after heat treatment.

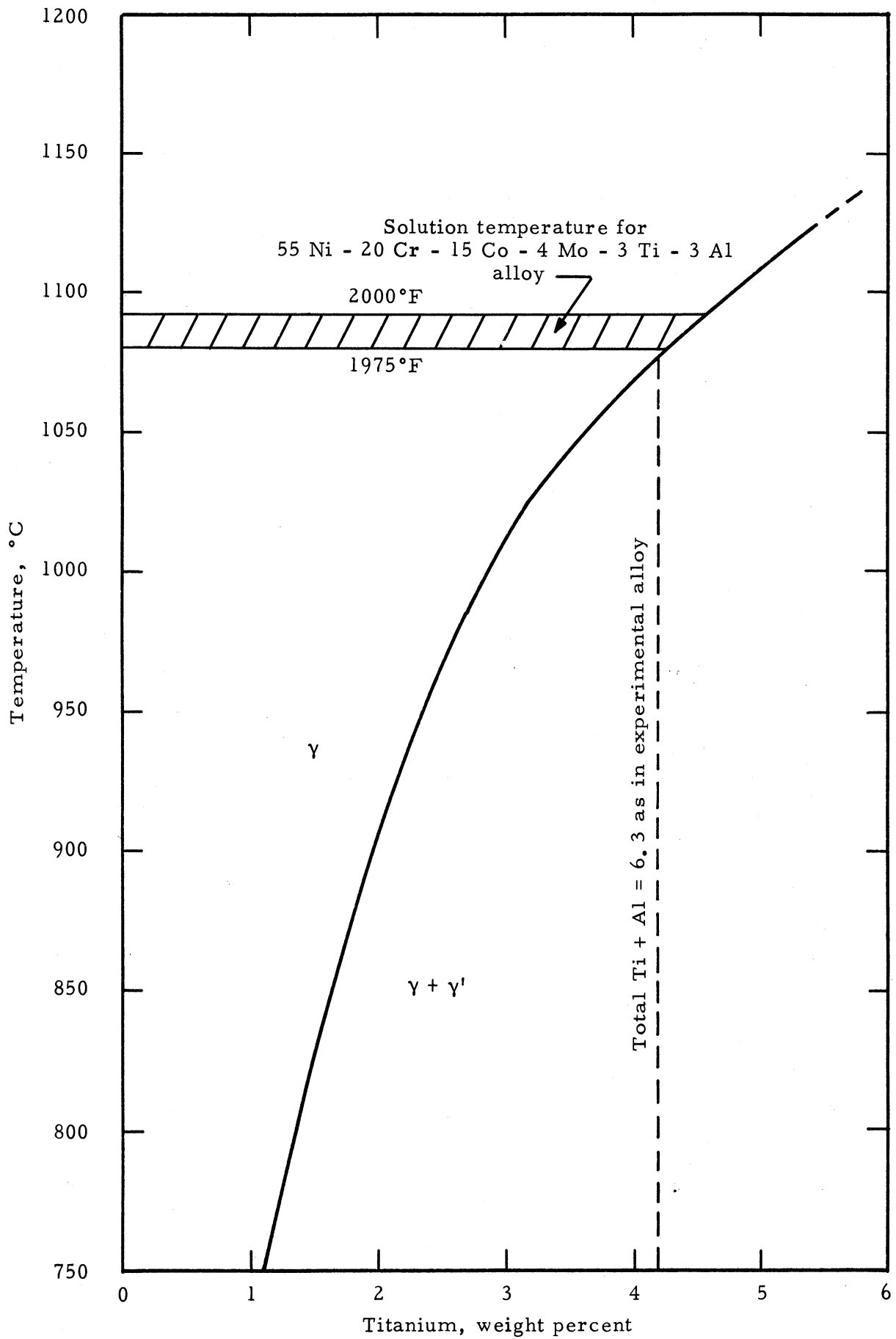
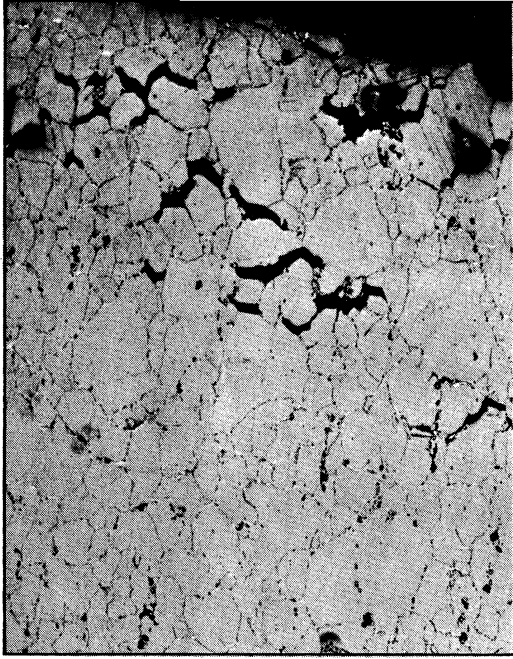


Figure 7. - Solution temperature of experimental 55 Ni - 20 Cr - 15 Co - 4 Mo - 3 Ti - 3 Al alloy plotted on data of Betteridge and Franklin (ref. 3). Curve is for 60 Ni - 20 Cr - 20 Co alloy with Ti/Al = 2/1.

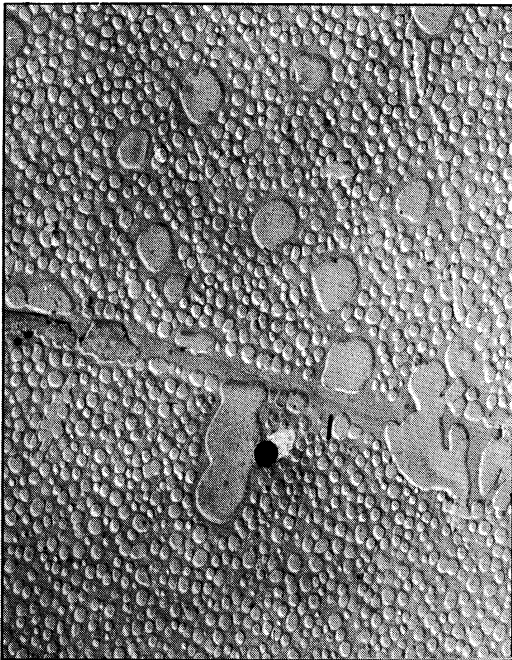


X100D

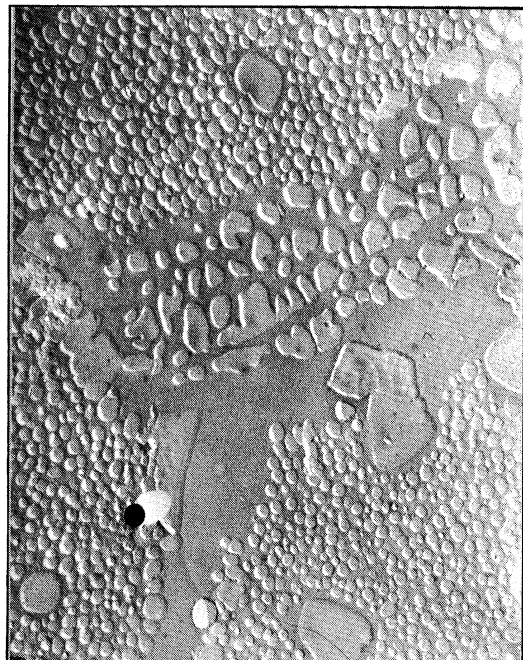


X1000D

(a) Optical micrographs near fracture.



X13,000D

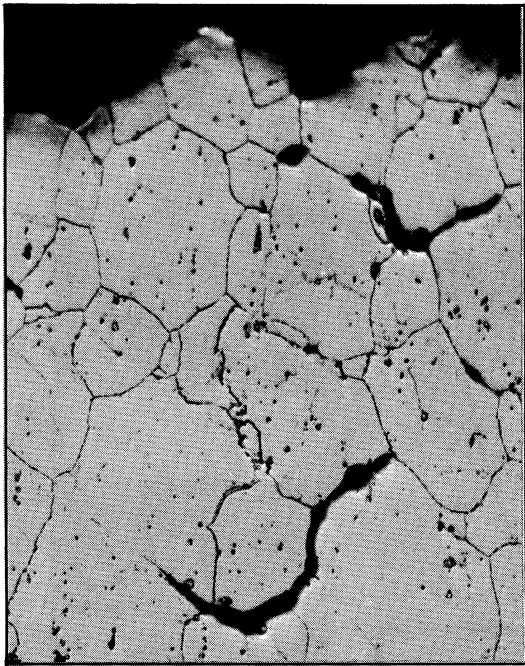


X13,000D

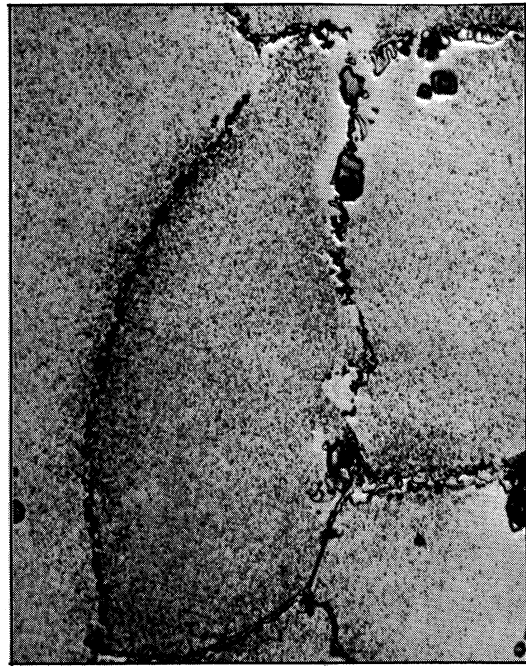
(b) Electron micrograph of lightly agglomerated grain boundary.

(c) Electron micrograph of heavily agglomerated grain boundary.

Figure 8. - Microstructure after rupture testing at 1600°F and 25,000 psi when prior heat treatment was 4 hours at 1975°F, air cooled. Hardness - 368 VPN; average rupture life - 60 hours.

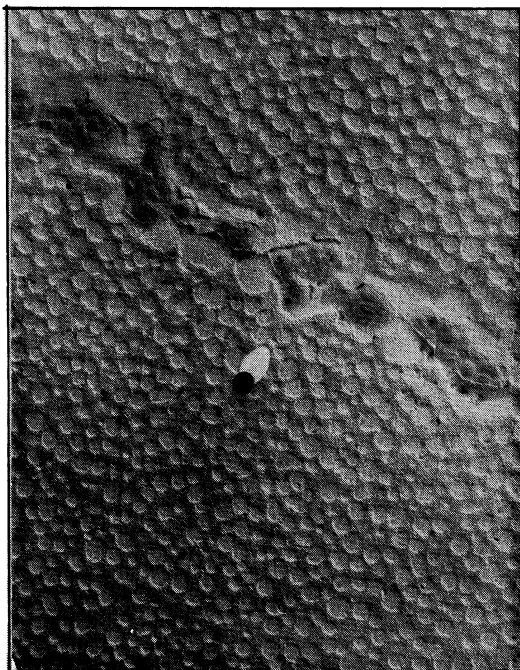


X100D

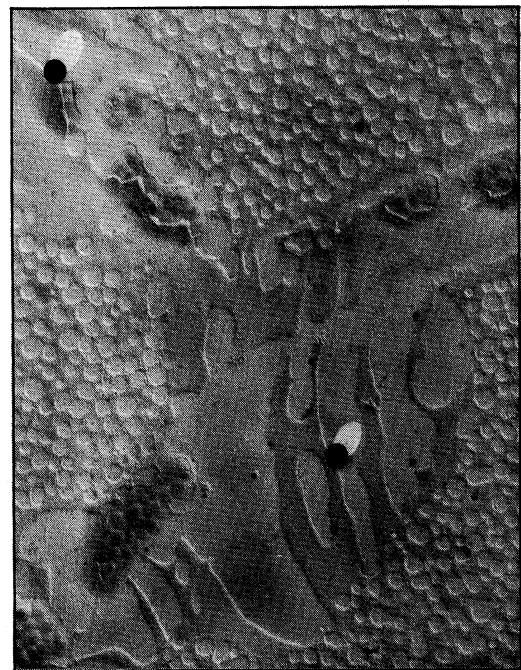


X1000D

(a) Optical micrograph near fracture.



X13,000D



X13,000D

(b) Electron micrograph of lightly agglomerated grain boundary.

(c) Electron micrograph of heavily agglomerated grain boundary.

Figure 9. - Microstructure after rupture testing at 1600°F and 25,000 psi when prior treatment was 2 hours at 2150°F, air cooled. Hardness - 365 VPN; average rupture life - 140 hours.

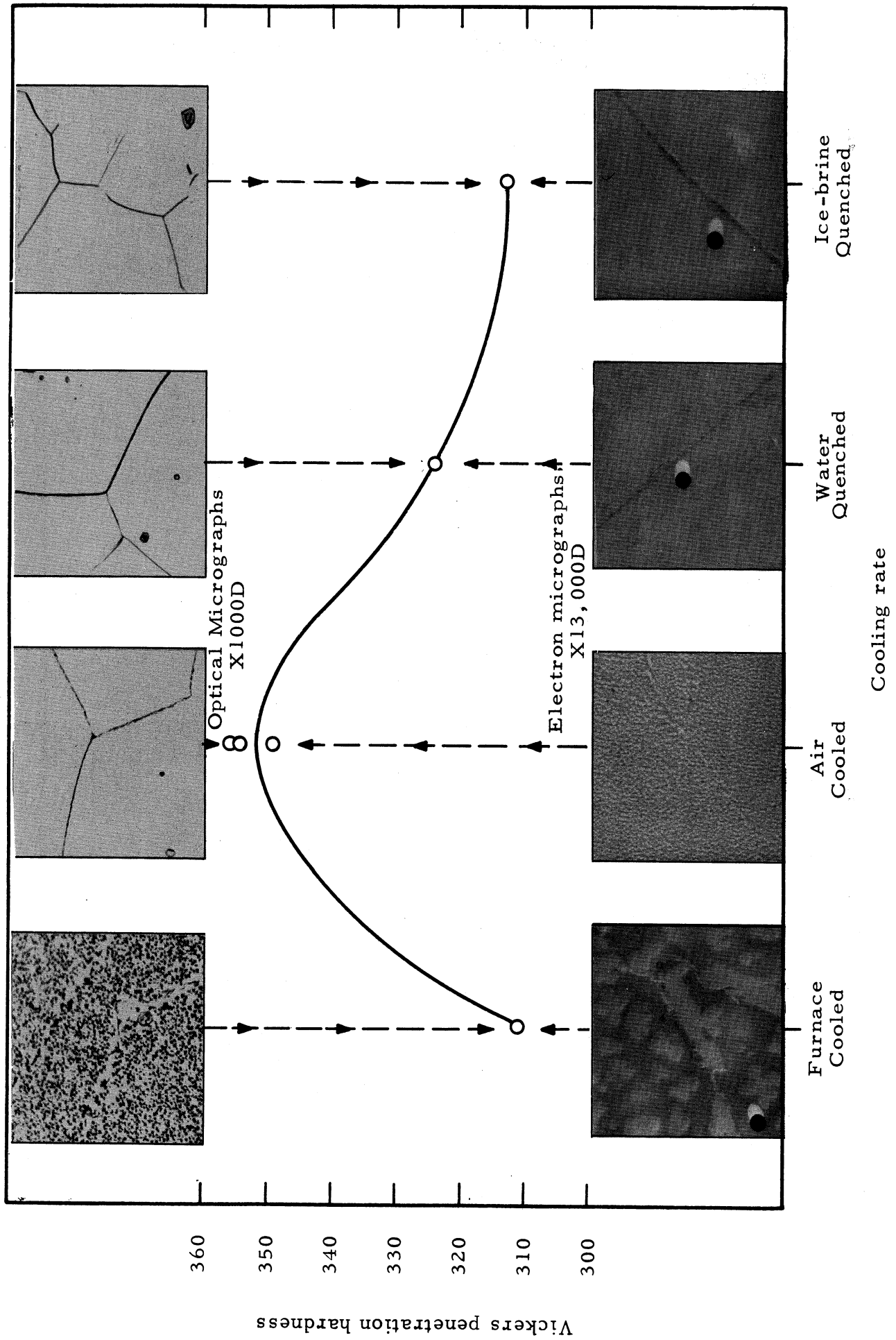
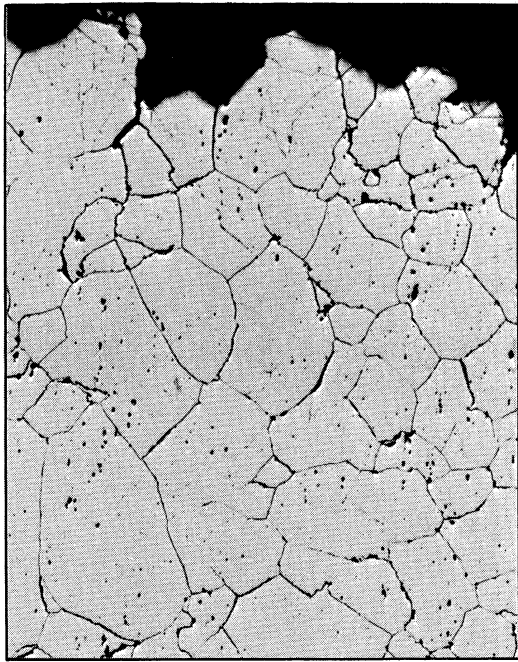


Figure 10. - Effect of cooling rate after heat treatment of 2 hours at 2150°F upon hardness and microstructure.

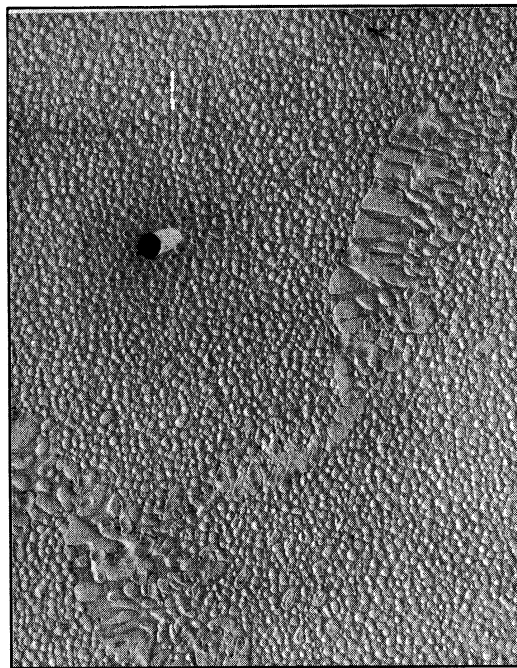


X100D



X1000D

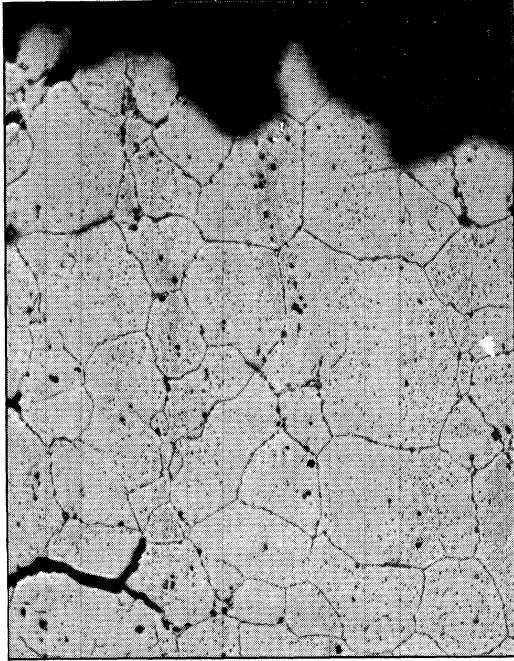
(a) Optical micrograph near fracture.



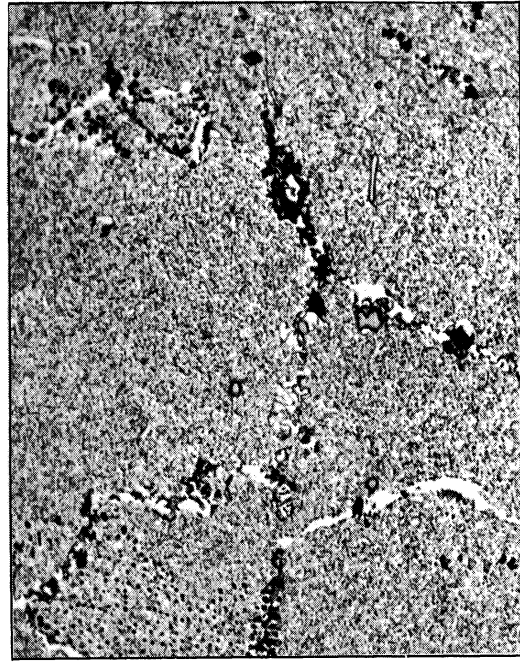
X13,000D

(b) Electron micrograph

Figure 11. - Microstructure after rupture testing at 1600°F and 25,000 psi when prior treatment was 2 hours at 2150°F, ice-brine quenched; plus 4 hours at 1975°F, ice-brine quenched; plus 24 hours at 1550°F, air cooled; plus 16 hours at 1400°F, air cooled. Hardness-402 VPN; rupture life - broke on loading.

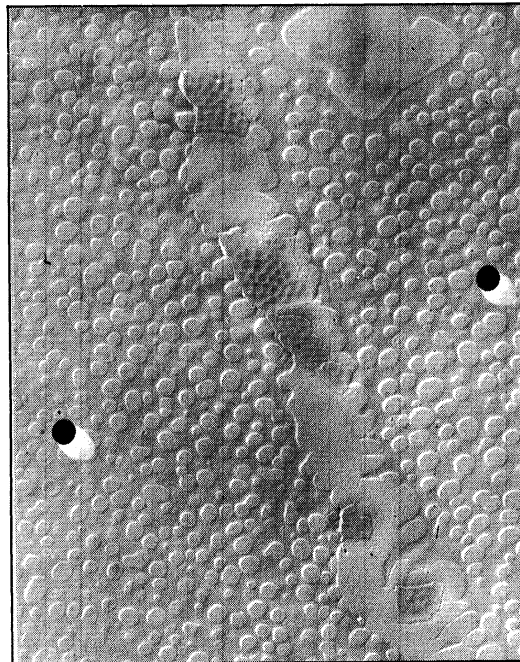


X100D



X1000D

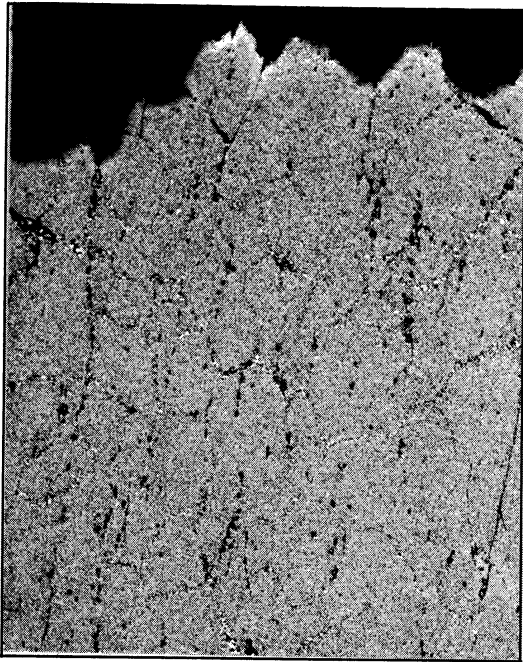
(a) Optical micrograph near fracture.



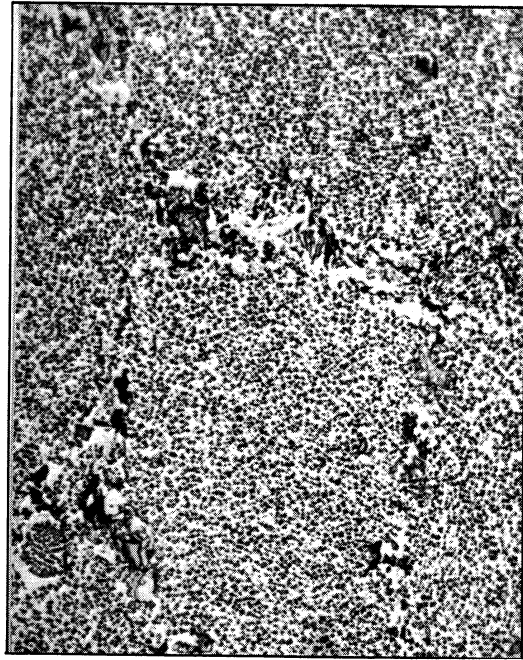
X13,000D

(b) Electron micrograph of lightly agglomerated grain boundary.

Figure 12. - Microstructure after rupture testing at 1600°F and 25,000 psi when prior treatment was 2 hours at 2150°F, air cooled; plus 4 hours at 1975°F, air cooled; plus 24 hours at 1550°F, air cooled; plus 16 hours at 1400°F, air cooled. Hardness-362 VP; rupture life - 152.9 hours.

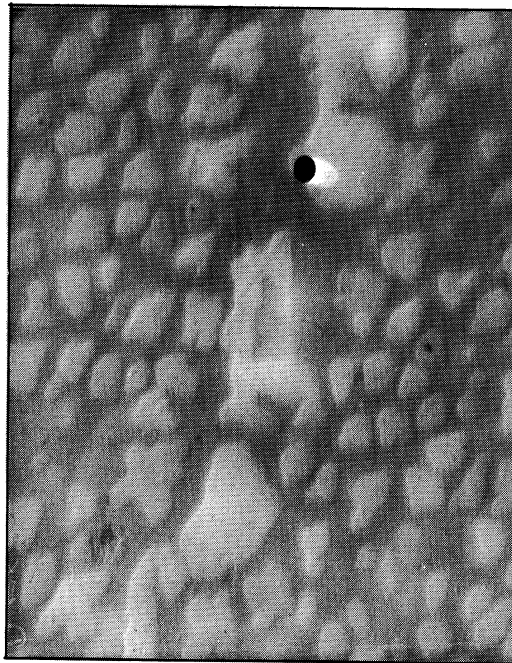


X100D



X 1000D

(a) Optical micrograph near fracture.



X13,000D

(b) Electron micrograph.

Figure 13.- Microstructure after rupture testing at 1600°F and 25,000 psi when prior treatment was 2 hours at 2150°F, furnace cooled. Hardness-325 VPN; average rupture life - 73 hours.



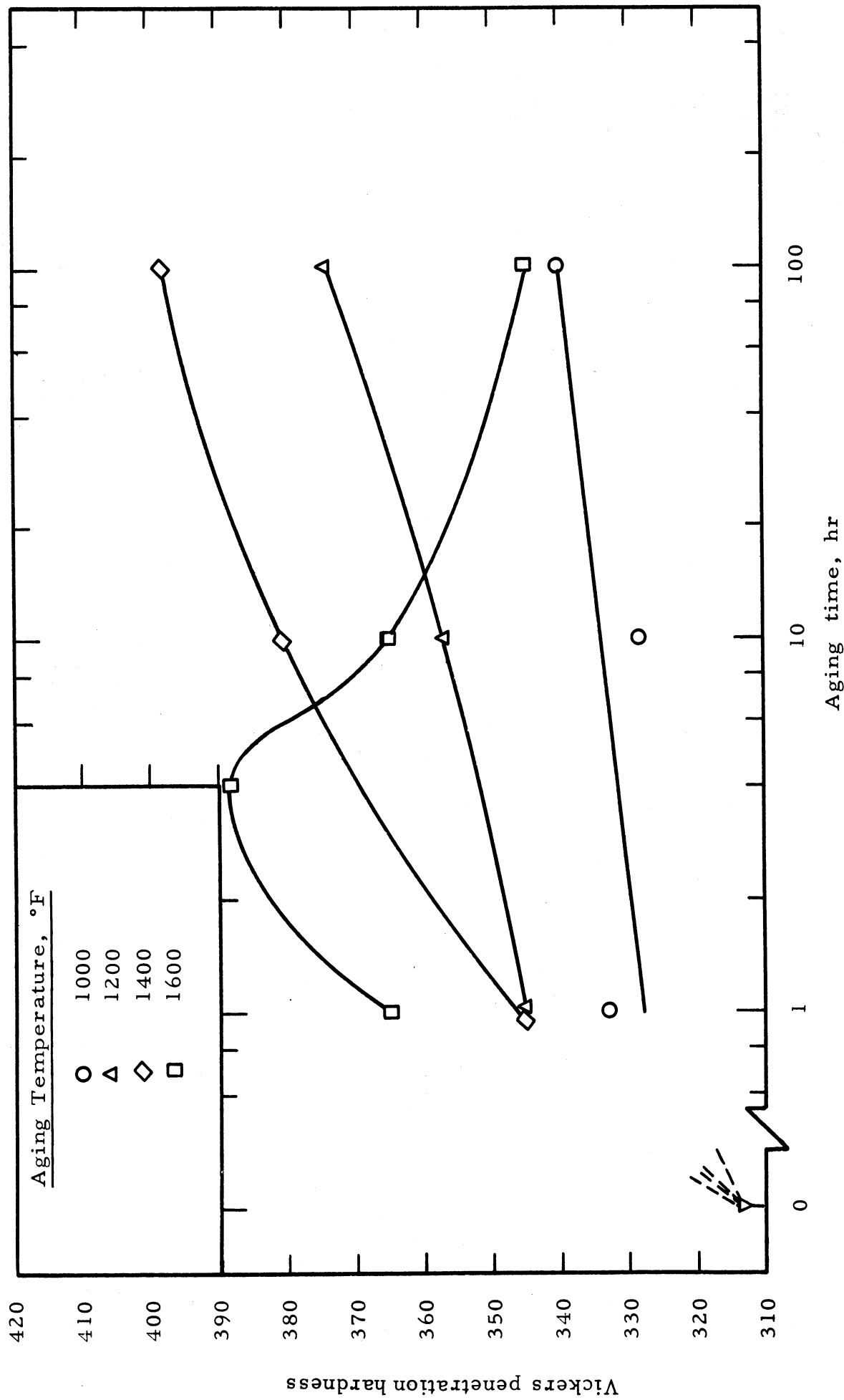


Figure 14.- Effect of aging temperature and time upon hardness. Treatment prior to aging was 2 hours at 2150°F, ice-brine quenched.

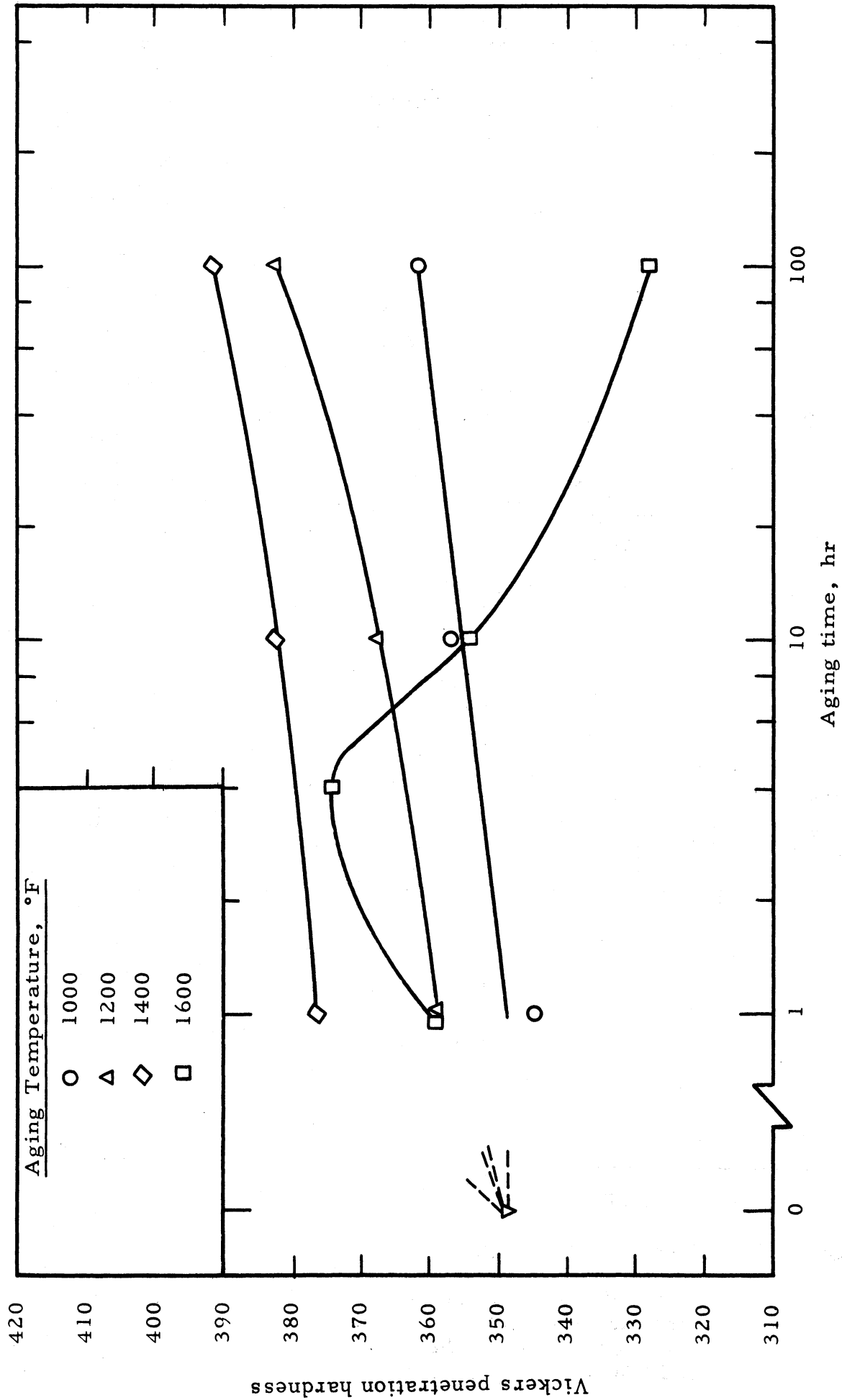
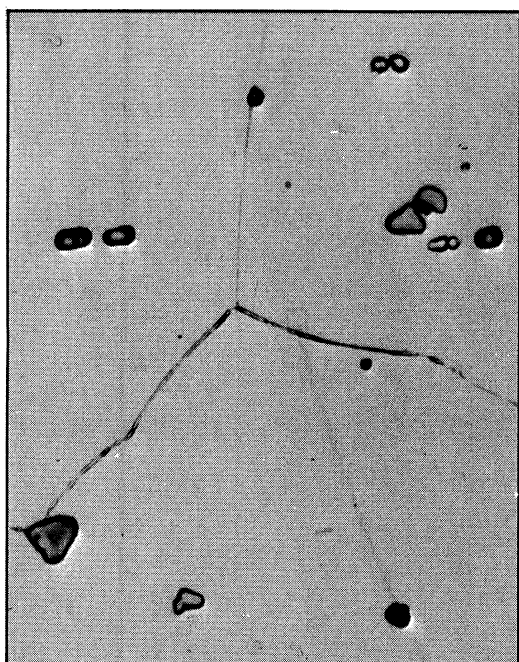
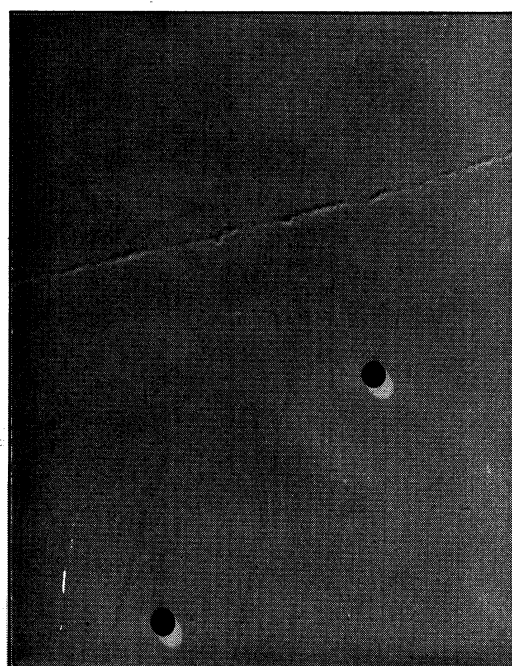


Figure 15.- Effect of aging temperature and time upon hardness. Treatment prior to aging was 2 hours at 2150°F, air cooled.



X1000D

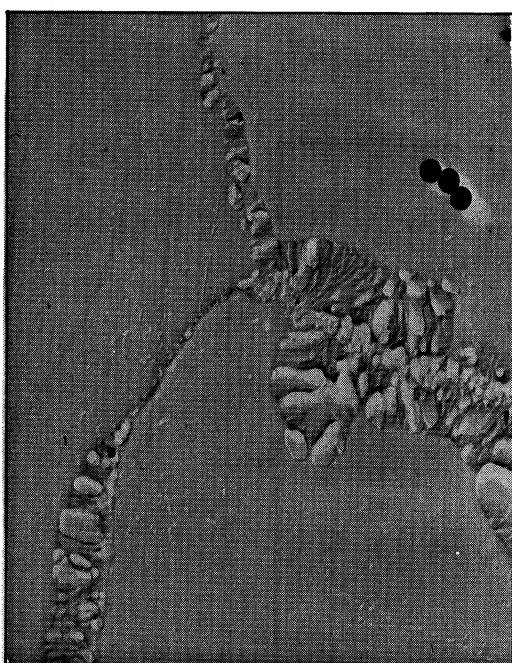


X13,000D

(a) 1000°F. Hardness -340 VPN.



X1000D



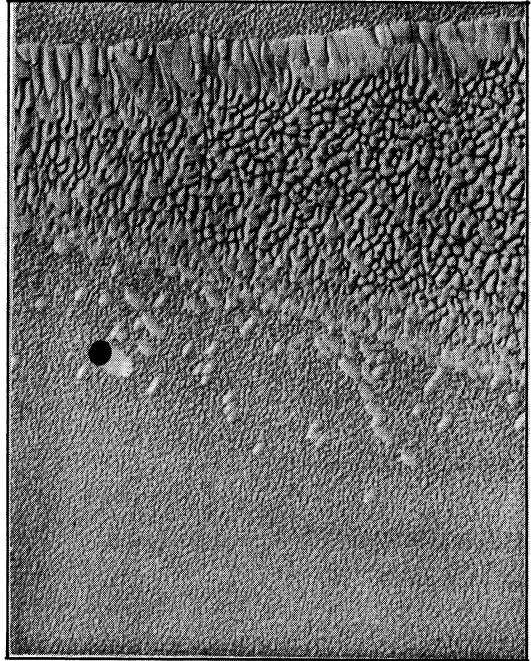
X13,000D

(b) 1200°F. Hardness -374 VPN.

Figure 16. - Effect of aging 100 hours at designated temperatures on the microstructure when initial treatment was 2 hours at 2150°F, ice-brine quenched. Micrographs at 1000D are optical micrographs; those at 13,000D are electron micrographs.

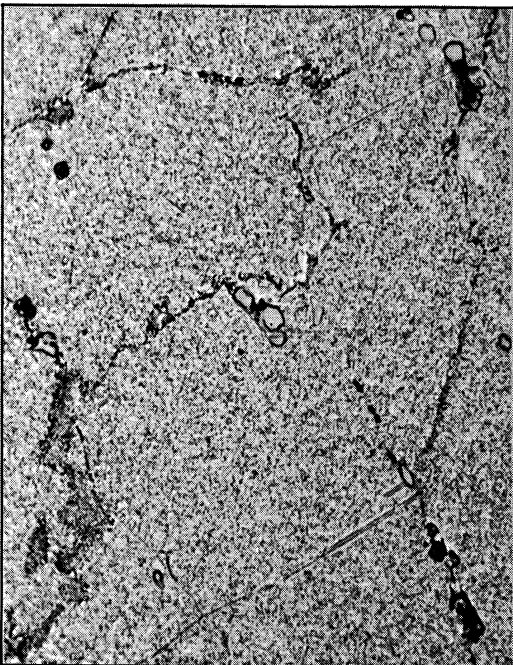


X1000D

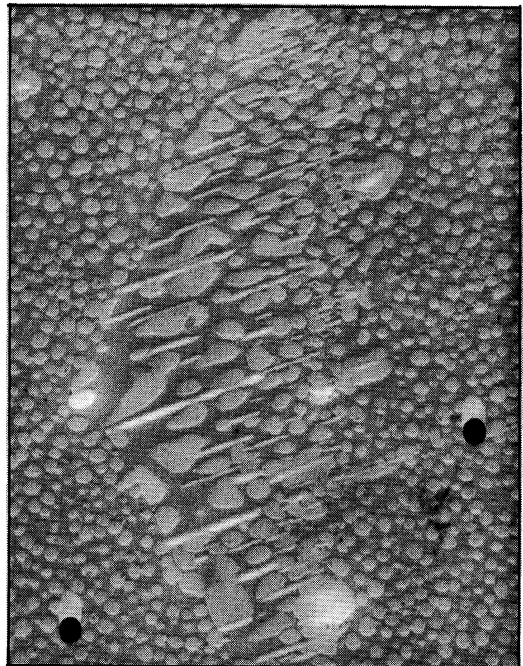


X13,000D

(c) 1400°F. Hardness-398 VPN.



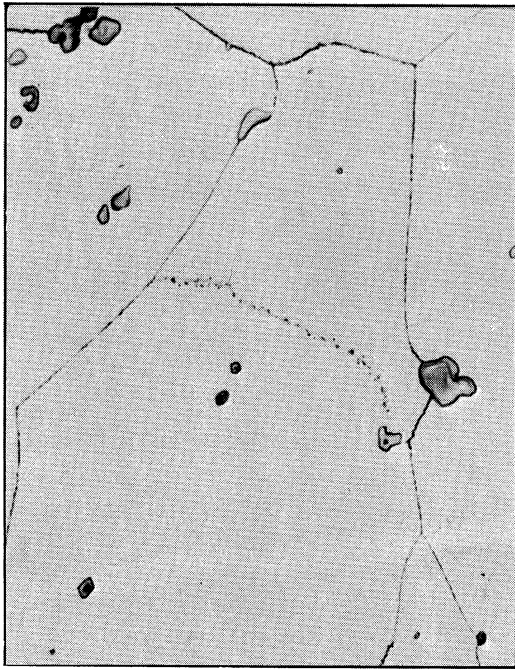
X1000D



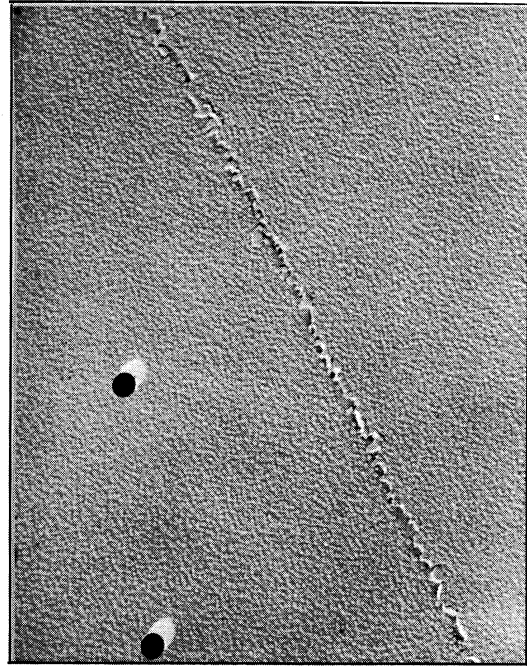
X13,000D

(d) 1600°F. Hardness-345 VPN.

Figure 16.- Concluded.



X1000D

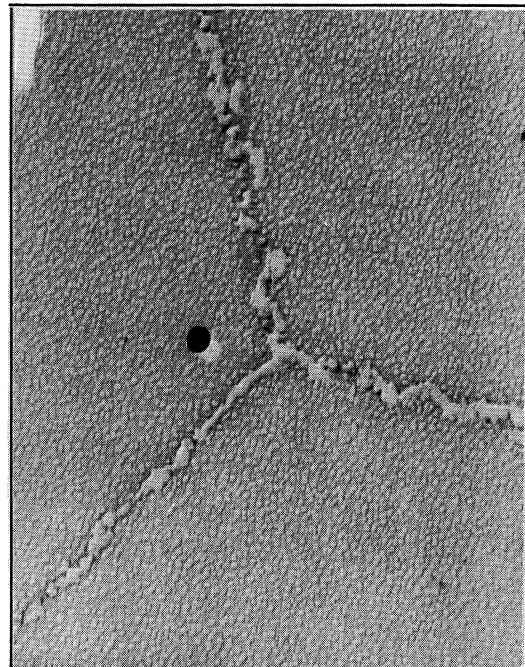


X13,000D

(a) 1000°F. Hardness-362 VPN.



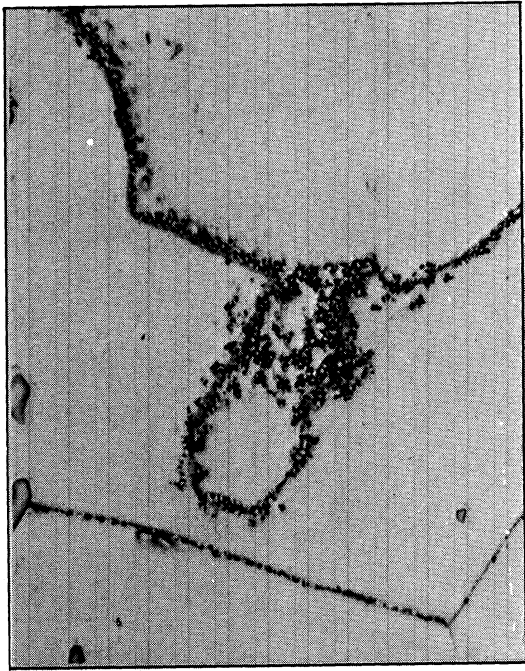
X1000D



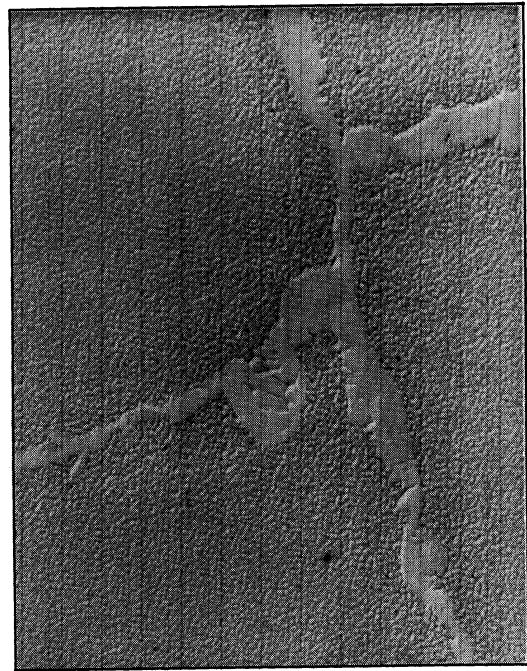
X13,000D

(b) 1200°F. Hardness-383 VPN.

Figure 17. - Effect of aging 100 hours at designated temperatures on the microstructure when initial treatment was 2 hours at 2150°F, air cooled. Micrographs at 1000D are optical micrographs; those at 13,000D are electron micrographs.



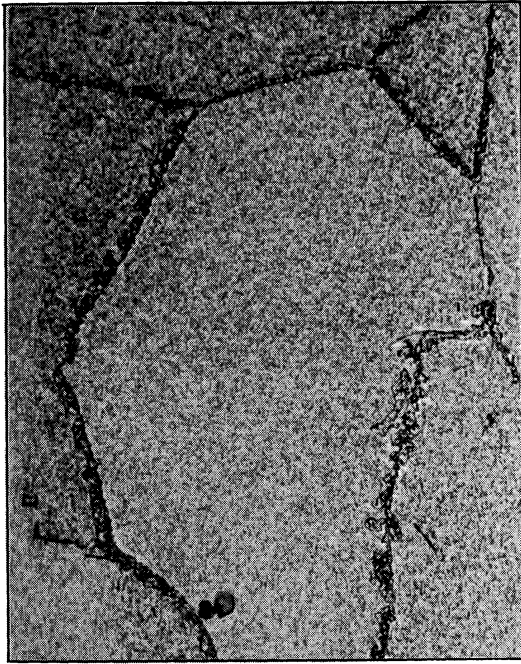
X1000D



X13,000D

(c) 1400°F. Hardness-392 VPN.

Figure 17.- Concluded.

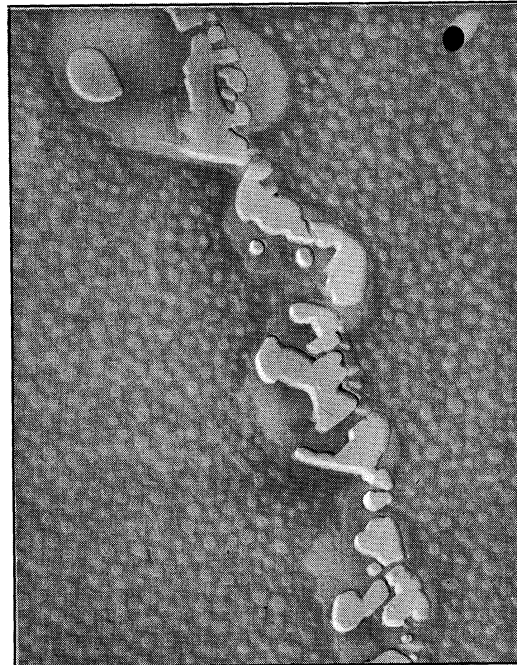


X1000D



X13,000D

(c) 100 hours. Hardness-328 VPN. The electron micrograph is with etchant B as were all others in the report except d, below.



X13,000D

(d) Same as c, with etchant C to reveal two-phase nature of grain boundary.

Figure 18. - Concluded.

## APPENDIX

### Analysis of Significance of Property Differences

Data from 45 hardness impressions and 50 rupture tests were analyzed to estimate testing scatter. The purpose of this was to establish if property differences obtained in the investigation were significant or if they could be accounted for by testing scatter alone.

For this analysis, the data were analyzed to establish the variance of test results,  $s^2$ , by using the following formula from Duncan (ref. 15):

$$s^2 = \frac{\sum (X - \bar{X})^2}{N - 1} \quad (1)$$

where

$s^2$  = variance of test results.

$X$  = test result.

$\bar{X}$  = average test result on samples.

$N$  = number of tests on each sample.

Once  $s^2$  had been established for the testing method for hardness or rupture life, the significance of differences in hardness or rupture times could be estimated using the difference test of Duncan (ref. 15) and the  $t$  distribution table:

$$t = \frac{\bar{X}_1 - \bar{X}_2}{s \sqrt{\frac{1}{N_1} + \frac{1}{N_2}}} \quad (2)$$

where

$t$  = value from table B, Duncan,  
using one tail test, 95% confidence limit.

$\bar{X}_1$  and  $\bar{X}_2$  = average test results on  
samples one and two.



$s = \sqrt{\text{variance of test results}}$

$N_1 = \text{number of tests on sample one.}$

$N_2 = \text{number of tests on sample two.}$

### Hardness

45 hardness impressions with two diagonal measurements per impression were used to calculate

$$s^2 = 9.65 \quad (3)$$

for a single diagonal measurement in ocular reading units.

Using the t distribution, the average diagonal measurement difference which was required for 95% confidence of a true hardness difference was

$$\bar{X}_1 - \bar{X}_2 = (t) \left( s \sqrt{\frac{1}{N_1} + \frac{1}{N_2}} \right) \quad (4)$$

with  $N_1$  and  $N_2 = 6$

$$\begin{aligned} \bar{X}_1 - \bar{X}_2 &= (1.67)(1.79) \\ &= 2.99 \end{aligned}$$

In the range of 300 to 340 VPN, 1 unit of ocular reading equals 2.35 VPN. Therefore, the difference in VPN between two specimens needed for 95% confidence of a true hardness difference was

$$(2.99)(2.35) = 7 \text{ VPN} \quad (5)$$

In the range of 340 to 400 VPN, 1 unit of ocular reading equals 3 VPN. Therefore, the difference in VPN between two specimens needed for 95% confidence of a true hardness difference was

$$(2.99)(3) = 9 \text{ VPN} \quad (6)$$

Therefore, when a greater difference than this was observed between the hardness of any two samples, the difference was considered significant.

## Rupture Life

50 stress-rupture tests were run at 1600°F and 25,000 psi. Two tests were run on each of 23 experimental heats of a 55 Ni - 20 Cr - 15 Co - 4 Mo - 3 Ti - 3 Al alloy and four tests were run on another heat. The average rupture life of these heats varied from 48.3 hours to 646.1 hours. The analysis yielded

$$s^2 = .00298 \quad (7)$$

as the variance of the log of the rupture life (in hours) of a rupture test.

Assuming that  $s^2$  does not vary with rupture life and using the t distribution, the difference of log rupture life which is required for 95% confidence of true strength differences was

$$\bar{X}_1 - \bar{X}_2 = (t) \left( s \sqrt{\frac{1}{N_1} + \frac{1}{N_2}} \right) \quad (8)$$

with  $N_1 = 2$  and  $N_2 = 2$

$$\begin{aligned} \bar{X}_1 - \bar{X}_2 &= (1.706)(.0545) \\ &= .093 \end{aligned}$$

Therefore, a difference of .093 in log rupture life between two conditions can be considered significant when  $N_1 = 2$  and  $N_2 = 2$ .

This has been applied to figure 4 by placing limits around the average rupture life for the 2 hours at 2150°F, air cooled treatment (B). These were calculated as 113 to 174 hours. When the average rupture life of two tests with another heat treatment fell outside these limits, this treatment was considered to give a significant change in high-temperature life from the life obtained with the 2 hours at 2150°F, air cooled treatment.

Heat treatments A and F in figure 4 were, therefore, considered to give inferior high-temperature life. Only one rupture test was needed for condition D to show the obvious inferiority. However, the rupture lives of the single tests run on conditions C, E and G were so close to condition B that additional tests were not needed to further show the comparability of properties.

